



HAL
open science

A theory of finite strain magneto-poromechanics

Boumediene Nedjar

► **To cite this version:**

Boumediene Nedjar. A theory of finite strain magneto-poromechanics. Journal of the Mechanics and Physics of Solids, 2015, 84, pp.293-312. 10.1016/j.jmps.2015.08.003 . hal-01188965

HAL Id: hal-01188965

<https://ensta-paris.hal.science/hal-01188965>

Submitted on 31 Aug 2015

HAL is a multi-disciplinary open access archive for the deposit and dissemination of scientific research documents, whether they are published or not. The documents may come from teaching and research institutions in France or abroad, or from public or private research centers.

L'archive ouverte pluridisciplinaire **HAL**, est destinée au dépôt et à la diffusion de documents scientifiques de niveau recherche, publiés ou non, émanant des établissements d'enseignement et de recherche français ou étrangers, des laboratoires publics ou privés.

A theory of finite strain magneto-poromechanics

B. Nedjar^a

^a*IMSIA, ENSTA ParisTech, CNRS, CEA, EDF,
Université Paris-Saclay,
828 bd des Maréchaux, 91762 Palaiseau, France*

Abstract

The main purpose of this paper is the multi-physics modeling of magnetically sensitive porous materials. We develop for this a magneto-poromechanics formulation suitable for the description of such a coupling. More specifically, we show how the current state of the art in the mathematical modeling of magneto-mechanics can easily be integrated within the unified framework of continuum thermodynamics of open media, which is crucial in setting the convenient forms of the state laws to fully characterize the behavior of porous materials. Moreover, due to the soft nature of these materials in general, the formulation is directly developed within the finite strain range. In a next step, a modeling example is proposed and detailed for the particular case of magneto-active foams with reversible deformations. In particular, due to their potentially high change in porosity, a nonlinear porosity law recently proposed is used to correctly describe the fluid flow through the interconnected pores when the solid skeleton is finitely strained causing fluid release or reabsorption. From the numerical point of view, the variational formulation together with an algorithmic design is described for an easy

Email address: boumediene.nedjar@ensta-paristech.fr (B. Nedjar)

implementation within the context of the finite element method. Finally, a set of numerical simulations is presented to illustrate the effectiveness of the proposed framework.

Keywords: Magneto-poromechanics, Continuum thermodynamics, Biot's theory, Large deformation, Magneto-active foams.

1. Introduction

Magneto-active polymers (MAPs) are mostly composites of a soft polymer matrix impregnated with magnetically permeable particles, typically iron particles in micro- or nano-meter size. In general, the response of MAPs to magnetic fields can be divided into two categories based on the property of the matrix material: they can give large and prompt deformation, or they can change their mechanical properties with moderate straining. These two features have received considerable attention in recent years due to their potential applications including, for instance, sensors, actuators, and bio-medicine, see for example Jolly et al. (1996); Zrínyi et al. (1996); Ginder et al. (2002); Varga et al. (2006) among many others.

In parallel, the mathematical modeling of the coupling of electromagnetic fields in deformable materials has also been an area of active research. Fully coupled nonlinear field theories have been developed with constitutive formulations based on augmented free energy functions, see for instance Dorfmann and Ogden (2004a); Ericksen (2006); Kankanala and Triantafyllidis (2004); Steigmann (2004); Vu and Steinmann (2007). In particular, it has been shown that any one of the magnetic induction, magnetic field, or magnetization vectors can be used as an independent variable for the magnetic part of

the problem, the other two being obtained through the constitutive relations. The relevant equations are based on the pioneering work of Pao (1978), see also Brown (1966); Kovetz (2000) for detailed discussions concerning these topics.

This work is devoted to the modeling of the particular case of magneto-active foams. These latter have a combination of desirable properties, including high porosity, light weight, low cost and fast responsiveness to external stimuli. Indeed, they have the ability to respond to magnetic fields with drastic change in volume, shape, and porosity. Furthermore, when the porosity is highly interconnected, they can be good candidates for biomedical systems used to control drug delivery, see Liu et al. (2006); Zhao et al. (2011), or to dynamically control flows in microfluidic chips, see Hong et al. (2014).

It becomes then of interest to develop a theory that couples the magnetic field with the large deformation in porous media. Historically, two approaches have been used in a relevant literature for the modeling of porous materials: mixture theories, see for example Bowen (1982); Wilmanski (2003), and the macroscale consolidation theory of Biot, see for example Biot (1941, 1972). The former approach is mostly used to model species migration where the mixture equations for mass balance are used in combination with classical equations for linear momentum balance in terms of rule-of-mixture relations for the stress response, see the recent examples of application in Duda et al. (2010); Baek and Pence (2011) among others. The present work is based on the latter approach, *i.e.* the Biot's theory. Since the pioneering work of Biot, considerable progress has been made in the last decades to develop a concise framework in the domain of poromechanics. Briefly, it describes

the evolution of a saturated porous material in terms of the deformation of its solid skeleton part in the one hand, and in terms of the distribution of the mass of its fluid part, on the other hand. The resulting boundary value problem consists of a coupling between the balance equation and the mass conservation of the fluid. The reader is referred for example to Lewis and Schrefler (1998); Coussy (2004) for a detailed synthesis.

The coupling with magnetostatics is integrated within the framework of continuum thermodynamics of open media for the correct setting of the whole set of constitutive relations. In particular, to describe the potentially high change of porosity, we use a simplified version of the porosity law recently proposed in Nedjar (2013a), see also Nedjar (2013b). This law accounts for the physical property that the actual (Eulerian) porosity must belong to the interval $[0, 1]$ for any admissible process as, by definition, the porosity is at any time a ratio of the connected porous space. Among others, this allows for a good description of the seepage process and the fluid release and/or absorption during the loading history.

A further goal of this paper is the formulation of a finite element treatment to furnish a computational tool for structural simulations. The three-field boundary value problem at hand being strongly coupled, it must be solved with the help of a combination of existing numerical strategies proposed in a relevant literature. As a very first attempt, we opt for a monolithic scheme where the three sub-problems are solved simultaneously. The most relevant particularities of the proposed numerical scheme are highlighted for an easy implementation.

An outline of the remainder of this paper is as follows. In Section 2, we

recall the governing equations of mass conservation and mechanical balance together with the specialized versions of Maxwell's equations. Both of the equivalent spatial and material descriptions are considered. Then, in Section 3, the magneto-mechanics coupling is embedded within the framework of continuum thermodynamics. In particular, we show how the formulation can be based on the magnetic induction vector or, equivalently, on the magnetic field vector. Section 4 is devoted to the modeling of hyperelastic magneto-active foams. Details of the whole constitutive equations are given together with the variational forms in view of the numerical approximation. This model example is then used for the simulations of Section 5. Finally, conclusions and perspectives are drawn in Section 6.

Notation: Throughout the paper, bold face characters refer to second- or fourth-order tensorial quantities. In particular, $\mathbf{1}$ denotes the second-order identity tensor with components δ_{ij} (δ_{ij} being the Kronecker delta), and \mathbf{I} is the fourth-order unit tensor of components $I_{ijkl} = \frac{1}{2}(\delta_{ik}\delta_{jl} + \delta_{il}\delta_{jk})$. The notation $(\cdot)^T$ is used for the transpose operator and the double dot symbol $\cdot\cdot$ is used for double tensor contraction, *i.e.* for any second-order tensors \mathbf{A} and \mathbf{B} , $\mathbf{A} : \mathbf{B} = \text{tr}[\mathbf{A}\mathbf{B}^T] = A_{ij}B_{ij}$ where, unless specified, summation on repeated indices is always assumed. One has the property $\text{tr}[(\cdot)] = (\cdot) : \mathbf{1}$ for the trace operator “tr”. The notation \otimes stands for the tensorial product. In components, one has $(\mathbf{A} \otimes \mathbf{B})_{ijkl} = A_{ij}B_{kl}$, and for any two vectors \mathbb{U} and \mathbb{V} , $(\mathbb{U} \otimes \mathbb{V})_{ij} = U_iV_j$. Furthermore, the double-striking characters will exclusively be used for vector fields related to the magnetic part of the problem, e.g. \mathbb{b} , \mathbb{B} , \mathbb{h}

2. Mass conservation and balance equations

When undeformed, unstressed, and in the absence of magnetic fields, the magnetically sensitive porous body occupies the reference configuration Ω_0 with boundary $\partial\Omega_0$. The porous body is thought as being a superimposition of a solid skeleton and a fluid phase. By solid skeleton, we mean the continuum formed from the constitutive matrix and the connected porous space emptied of fluid. Its deformation is the one that is observable under the combined action of mechanical forces and magnetic fields.

We identify a material solid skeleton particle by its position vector in the reference configuration, $\mathbf{X} \in \Omega_0$, and trace its motion by its current position at time t , $\mathbf{x}(\mathbf{X}, t) \in \Omega_t$. The deformation gradient is as usual defined as $\mathbf{F} = \nabla_{\mathbf{X}} \mathbf{x}$, where $\nabla_{\mathbf{X}}(\cdot)$ is the material gradient operator with respect to the reference coordinates \mathbf{X} . The Jacobian of the transformation is given by the determinant $J = \det \mathbf{F}$ with the standard convention $J > 0$.

Furthermore, for the porous space, we denote by n the Eulerian porosity which is the volume fraction of the connected porous space in the spatial configuration. Thus, for a current elementary volume $d\Omega_t$ of porous material, the volume of porous space within it is $nd\Omega_t$.

Now in contrast to the Eulerian porosity, the change in the porous space is thermodynamically better captured relative to the reference configuration through the Lagrangian porosity that we denote here by ϕ . This latter is defined by the following Piola transform: If $d\Omega_0$ is the reference elementary volume to which $d\Omega_t$ corresponds, the relation $\phi d\Omega_0 = nd\Omega_t$ holds. Hence, as the relation between the elementary reference and current volumes is given by

$d\Omega_t = Jd\Omega_0$, we thereby get the important relation between the Lagrangian and Eulerian porosities

$$\phi = Jn \quad (1)$$

2.1. Mass conservation for open systems

Within a spatial elementary volume $d\Omega_t$, the current fluid mass content is $\rho_f n d\Omega_t$, where ρ_f is the actual fluid density. Likewise, the current solid mass content is $\rho_s(1 - n)d\Omega_t$, where ρ_s is the actual density of the matrix that constitutes the solid skeleton. Therefore, by distinguishing the material time derivative with respect to the solid phase $d^s(\cdot)/dt$ from the one relative to the fluid phase $d^f(\cdot)/dt$, the Eulerian forms of the mass conservations for the solid and fluid phases are respectively given by:

$$\frac{d^s}{dt} \int_{\Omega_t} \rho_s(1 - n) d\Omega_t = 0 \quad \text{and} \quad \frac{d^f}{dt} \int_{\Omega_t} \rho_f n d\Omega_t = 0 \quad (2)$$

for any partial or total volume Ω_t of porous material. Furthermore, the fluid mass conservation (2)₂ rewritten in terms of the material time derivative with respect to the solid phase is equivalently given by (see Appendix A for details),

$$\frac{d^s}{dt} \int_{\Omega_t} \rho_f n d\Omega_t = - \int_{\Omega_t} \text{div} \mathbf{q}_f d\Omega_t \quad (3)$$

where \mathbf{q}_f is the spatial flow vector of fluid mass, and given by

$$\mathbf{q}_f = \rho_f \boldsymbol{\nu} \quad \text{with} \quad \boldsymbol{\nu} = n(\mathbf{v}_f - \mathbf{v}_s) \quad (4)$$

for the filtration vector $\boldsymbol{\nu}$, and the relative velocity $(\mathbf{v}_f - \mathbf{v}_s)$ of the fluid with respect to the velocity of the solid skeleton \mathbf{v}_s , see the sketch of Figure 1 for an illustration. In Eq. (3), $\text{div}(\cdot)$ is the divergence operator with respect to the

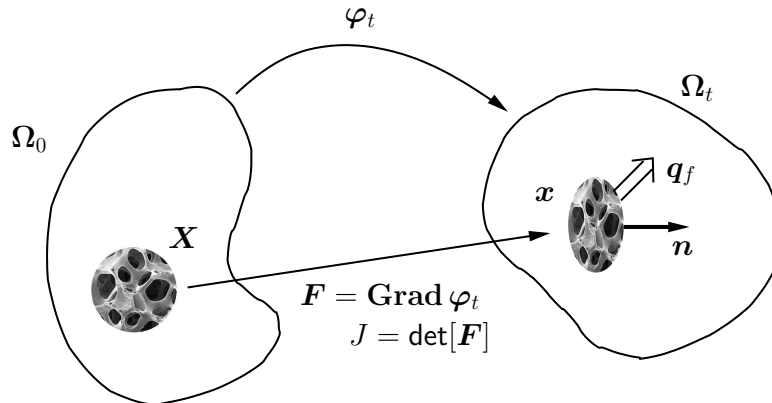


Figure 1: A magneto-active porous solid under a deformation φ_t of the solid skeleton and a fluid flow characterized by the flow vector \mathbf{q}_f .

spatial coordinates \mathbf{x} . It is denoted by $\text{Div}(\cdot)$ in the material configuration with respect to \mathbf{X} .

Furthermore, relative to the reference configuration, we introduce the Lagrangian fluid mass content, denoted here by M_f , and defined per unit of reference volume $d\Omega_0$. It is related to the current fluid mass content per unit of current volume $d\Omega_t$ as: $M_f d\Omega_0 = \rho_f n d\Omega_t$. On the one hand, one obtains the well-known definition

$$M_f = \rho_f \phi \quad (5)$$

where use has been made of the relation (1), and on the other hand, the spatial fluid mass conservation (3) leads to the following local Lagrangian form

$$\dot{M}_f = -\text{Div}\mathbf{Q}_f \quad (6)$$

where \mathbf{Q}_f is the material flow vector of fluid mass related to its spatial counterpart \mathbf{q}_f via the Piola transform $\mathbf{Q}_f = J\mathbf{F}^{-1}\mathbf{q}_f$. In Eq. (6) and

henceforth, the dot operator $(\dot{\cdot})$ is the material time derivative with respect to the solid phase which reduces to a simple derivative with respect to time for a Lagrangian quantity.

2.2. Magnetostatics equations

As the porous materials we consider are electrically non-conducting, the magnetostatic fields are governed by the following specializations of Maxwell's equations in the absence of distributed currents and time dependence

$$\begin{aligned} \text{Ampère's law:} \quad \text{curl } \mathfrak{h} &= \mathbf{0} \quad \text{in } \Omega_t \\ \text{Gauss's law:} \quad \text{div } \mathfrak{b} &= 0 \quad \text{in } \Omega_t \end{aligned} \tag{7}$$

where \mathfrak{h} and \mathfrak{b} are respectively the magnetic field and magnetic induction vectors, both with respect to the spatial configuration. They are related by the standard relation

$$\mathfrak{b} = \mu_0 (\mathfrak{h} + \mathfrak{m}) \tag{8}$$

where \mathfrak{m} is the spatial magnetization vector. The constant μ_0 is the magnetic permeability of vacuum. In Eq. (7)₁, $\text{curl}(\cdot)$ denotes the rotational operator with respect to \mathbf{x} . It is denoted by $\text{Curl}(\cdot)$ in the material configuration with respect to \mathbf{X} .

Pull-back to the reference configuration gives the Lagrangian counterparts of the above laws:

$$\text{Curl } \mathbb{H} = \mathbf{0} \quad \text{and} \quad \text{Div } \mathbb{B} = 0 \quad \text{in } \Omega_0 \tag{9}$$

for the Piola transforms

$$\mathbb{H} = \mathbf{F}^T \mathfrak{h} \quad \mathbb{B} = J \mathbf{F}^{-1} \mathfrak{b} \quad \mathbb{M} = \mathbf{F}^T \mathfrak{m} \tag{10}$$

Using the relation (8), the Lagrangian magnetic induction vector given by Eq. (10)₂ becomes

$$\mathbb{B} = \mu_0 J \mathbf{C}^{-1} (\mathbb{H} + \mathbb{M}) \quad (11)$$

where $\mathbf{C} = \mathbf{F}^T \mathbf{F}$ is the right Cauchy-Green tensor which, otherwise, is a strain measure for the solid skeleton.

2.3. Mechanical balance and power of external forces

The magneto-active porous materials we have in mind are those where only the solid skeleton is sensitive to external magnetic fields. This fact is here taken into account within the classical Biot's theory. In statics, the spatial forms of the partial balance equations are given by

$$\begin{aligned} \operatorname{div}((1-n)\boldsymbol{\sigma}_s) + \mathbb{f}_m + \rho_s(1-n)\mathbf{f} + \mathbf{f}_{\text{int}}^s &= \mathbf{0} & \text{in } \Omega_t, \\ (1-n)\boldsymbol{\sigma}_s \mathbf{n} &= \mathbf{t}_s & \text{on } \partial\Omega_t \end{aligned} \quad (12)$$

for the solid skeleton, and

$$\begin{aligned} \operatorname{div}(n\boldsymbol{\sigma}_f) + \rho_f n \mathbf{f} + \mathbf{f}_{\text{int}}^f &= \mathbf{0} & \text{in } \Omega_t, \\ n\boldsymbol{\sigma}_f \mathbf{n} &= \mathbf{t}_f & \text{on } \partial\Omega_t \end{aligned} \quad (13)$$

for the fluid phase.

In these equations, $\boldsymbol{\sigma}_s$ and $\boldsymbol{\sigma}_f$ are respectively the partial Cauchy stress tensors relative to the solid skeleton and to the fluid phase, \mathbf{t}_s and \mathbf{t}_f are the respective prescribed Cauchy traction vectors on the boundary $\partial\Omega_t$ of unit outer normal \mathbf{n} , \mathbf{f} is the volumetric body force, and $\mathbf{f}_{\text{int}}^s$ and $\mathbf{f}_{\text{int}}^f$ are macroscopic interaction forces exerted by the other continuum. These latter are such that $\mathbf{f}_{\text{int}}^s + \mathbf{f}_{\text{int}}^f = \mathbf{0}$. And last, \mathbb{f}_m is the magnetic body force per unit volume that *solely* affects the solid skeleton's partial mechanical balance. It

is given by $\mathbb{f}_m = [\nabla_{\mathbf{x}} \mathbb{b}]^T \mathbf{m}$, see for example Pao (1978). Here and in all what follows, the notation $\nabla_{\mathbf{x}}(\cdot)$ refers to the spatial gradient operator with respect to the coordinates \mathbf{x} . Adding up both contributions, we get the balance equation

$$\operatorname{div} \boldsymbol{\sigma} + \mathbb{f}_m + \rho \mathbf{f} = \mathbf{0} \quad \text{in } \Omega_t \quad (14)$$

with

$$\boldsymbol{\sigma} = (1 - n)\boldsymbol{\sigma}_s + n\boldsymbol{\sigma}_f \quad \text{and} \quad \rho = (1 - n)\rho_s + n\rho_f \quad (15)$$

for the total Cauchy stress tensor $\boldsymbol{\sigma}$ and the current density ρ of the porous material. Notice that due to the magnetization, the partial stress $\boldsymbol{\sigma}_s$ is in general non-symmetric, and so is the total stress $\boldsymbol{\sigma}$. Nevertheless, we adopt here the well known structure where the stress is augmented with terms arising from the magnetic body force. Indeed, this latter can equivalently be written as, see for example Dorfmann and Ogden (2004a), Steigmann (2004), and Vu and Steinmann (2007),

$$\mathbb{f}_m = \operatorname{div} \left(\underbrace{\mu_0^{-1} \left[\mathbb{b} \otimes \mathbb{b} - \frac{1}{2} \mathbb{b} \cdot \mathbb{b} \mathbf{1} \right] + \mathbf{m} \cdot \mathbb{b} \mathbf{1} - \mathbf{m} \otimes \mathbb{b}}_{= \boldsymbol{\sigma}_m} \right) \quad (16)$$

where we have introduced for convenience the notation $\boldsymbol{\sigma}_m$ for the magnetic interaction stress tensor. The balance equation (14) can then equivalently be written as

$$\operatorname{div} \tilde{\boldsymbol{\sigma}} + \rho \mathbf{f} = \mathbf{0} \quad \text{in } \Omega_t \quad (17)$$

in terms of the augmented¹ Cauchy stress tensor $\tilde{\boldsymbol{\sigma}}$ defined by $\tilde{\boldsymbol{\sigma}} = \boldsymbol{\sigma} + \boldsymbol{\sigma}_m$. The stress $\tilde{\boldsymbol{\sigma}}$ is this time symmetric. The pull-back of the balance equation

¹Note that in the literature the widely used term is *total stress*, e.g. Bustamante et al. (2006). Here we prefer to use the term *augmented stress* instead. The term *total* is left to

(17) to the reference configuration gives the following useful Lagrangian form

$$\text{Div } \tilde{\mathbf{P}} + \rho_0 \mathbf{f} = \mathbf{0} \quad \text{in } \Omega_0 \quad (18)$$

in terms of the augmented first Piola-Kirchhoff stress tensor $\tilde{\mathbf{P}} \equiv \mathbf{F}\tilde{\mathbf{S}} = J\tilde{\boldsymbol{\sigma}}\mathbf{F}^{-T}$ and the reference density $\rho_0 = J\rho$, $\tilde{\mathbf{S}}$ being the augmented second Piola-Kirchhoff stress tensor. In particular, the first Piola-Kirchhoff magnetic interaction part $\mathbf{P}_m = J\boldsymbol{\sigma}_m\mathbf{F}^{-T}$ is

$$\mathbf{P}_m = \frac{1}{\mu_0 J} \left[\mathbf{F}\mathbb{B} \otimes \mathbb{B} - \frac{1}{2} \mathbf{C} : \mathbb{B} \otimes \mathbb{B} \mathbf{F}^{-T} \right] + \mathbb{M} \cdot \mathbb{B} \mathbf{F}^{-T} - \mathbf{F}^{-T} \mathbb{M} \otimes \mathbb{B} \quad (19)$$

where use has been made of the relations (10)₂ and (10)₃.

For later use, let us compute the power of the external forces, \mathcal{P}_{ext} , for the open system at hand. Adding up the contributions of both phases, it is given by

$$\begin{aligned} \mathcal{P}_{\text{ext}} &= \int_{\Omega_t} (\rho_s(1-n)\mathbf{f} + \mathbb{f}_m + \mathbf{f}_{\text{int}}^s) \cdot \mathbf{v}_s + (\rho_f n \mathbf{f} + \mathbf{f}_{\text{int}}^f) \cdot \mathbf{v}_f \, d\Omega_t \\ &\quad + \int_{\partial\Omega_t} \mathbf{t}_s \cdot \mathbf{v}_s + \mathbf{t}_f \cdot \mathbf{v}_f \, da \end{aligned} \quad (20)$$

Use of the divergence theorem after having replaced the boundary traction vectors (12)₂ and (13)₂, use of the relations (15), and simplifying with the balance equation (14), we get

$$\mathcal{P}_{\text{ext}} = \int_{\Omega_t} \boldsymbol{\sigma} : \nabla_x \mathbf{v}_s + \mathbf{f} \cdot \mathbf{q}_f + \text{div} (n \boldsymbol{\sigma}_f^T (\mathbf{v}_f - \mathbf{v}_s)) + \mathbf{f}_{\text{int}}^f \cdot (\mathbf{v}_f - \mathbf{v}_s) \, d\Omega_t$$

where the relation (4) for the spatial flow vector of fluid mass \mathbf{q}_f has been used. Furthermore, as the fluid partial stress tensor $\boldsymbol{\sigma}_f$ can be addressed

its classical meaning in poromechanics; the additional contributions of the solid skeleton and the fluid phase, *i.e.* the total stress $\boldsymbol{\sigma}$ defined in Eq. (15)₁.

through a spherical tensor, we henceforth adopt the form $\boldsymbol{\sigma}_f = -p\mathbf{1}$ for the fluid pore pressure p . Finally, giving ride of the term $\mathbf{f}_{\text{int}}^f \cdot (\mathbf{v}_f - \mathbf{v}_s)$ to the benefit of the fluid pore pressure, we end up with the form that will be used in the following thermodynamic developments

$$\mathcal{P}_{\text{ext}} = \int_{\Omega_t} \boldsymbol{\sigma} : \nabla_{\mathbf{x}} \mathbf{v}_s + \mathbf{f} \cdot \mathbf{q}_f - \text{div} \left(\frac{p}{\rho_f} \mathbf{q}_f \right) d\Omega_t \quad (21)$$

where the relation (4) has again been used. In Eq. (21), $\nabla_{\mathbf{x}} \mathbf{v}_s$ is the spatial velocity gradient of the solid skeleton that is related to the deformation gradient through the well known kinematic relation $\nabla_{\mathbf{x}} \mathbf{v}_s = \dot{\mathbf{F}} \mathbf{F}^{-1}$.

3. Continuum thermodynamics and constitutive equations

The above governing equations need now to be supplemented with adequate constitutive relations. These latter together with the characterization of the dissipation phenomena are constructed in accordance with the requirements of continuum thermodynamics. We demonstrate in this work how the current state of the art in magneto-mechanics can be embedded within the up to date poromechanics developments in a straightforward manner.

3.1. First principle: energy conservation

With respect to the spatial configuration, the first law of thermodynamics for our magneto-sensitive open system is given by

$$\frac{d^s}{dt} \int_{\Omega_t} \rho_s (1 - n) e_s d\Omega_t + \frac{d^f}{dt} \int_{\Omega_t} \rho_f n e_f d\Omega_t = \mathcal{P}_{\text{ext}} + \mathcal{Q} + \mathcal{P}_m \quad (22)$$

where e_s and e_f are the specific, *i.e.* per unit of mass, internal energies of the solid skeleton's constitutive matrix and the fluid phase, respectively. While

the power of the external forces \mathcal{P}_{ext} is given by Eq. (21), \mathcal{Q} is the thermal flux power and \mathcal{P}_m is the magnetic power, respectively given by

$$\mathcal{Q} = \int_{\partial\Omega_t} -\mathbf{q} \cdot \mathbf{n} \, da \quad \text{and} \quad \mathcal{P}_m = \int_{\Omega_t} -\text{m} \cdot \frac{d^s \mathbb{b}}{dt} \, d\Omega_t \quad (23)$$

where \mathbf{q} is the spatial heat flux vector. The left hand side of Eq. (22) can be rewritten as

$$\int_{\Omega_t} \frac{d^s e}{dt} + e \operatorname{div} \mathbf{v}_s + \operatorname{div}(e_f \mathbf{q}_f) \, d\Omega_t \quad (24)$$

where $e = \rho_s(1-n)e_s + \rho_f n e_f$ is the total *volumetric* internal energy of the porous material. With Eqs. (24), (21) and (23), the energy conservation (22) is rewritten as

$$\int_{\Omega_t} \frac{d^s e}{dt} + e \operatorname{div} \mathbf{v}_s \, d\Omega_t = \int_{\Omega_t} \boldsymbol{\sigma} : \nabla_{\mathbf{x}} \mathbf{v}_s - \operatorname{div}(h_f \mathbf{q}_f + \mathbf{q}) + \mathbf{f} \cdot \mathbf{q}_f - \text{m} \cdot \frac{d^s \mathbb{b}}{dt} \, d\Omega_t \quad (25)$$

where $h_f = e_f + p/\rho_f$ is the specific enthalpy of the fluid, see Appendix B for useful details. Hence, the local form of the first law is given by

$$\frac{d^s e}{dt} + e \operatorname{div} \mathbf{v}_s = \boldsymbol{\sigma} : \nabla_{\mathbf{x}} \mathbf{v}_s - \operatorname{div}(h_f \mathbf{q}_f + \mathbf{q}) + \mathbf{f} \cdot \mathbf{q}_f - \text{m} \cdot \frac{d^s \mathbb{b}}{dt} \quad (26)$$

which should be compared with the corresponding one for closed systems, see for example Pao (1978); Brigadnov and Dorfmann (2003).

However, for the following developments, the Lagrangian form is better suited. The energy conservation (25) must then be pull-back to the reference configuration. Denoting by E the material total internal energy per unit reference volume of the solid skeleton such that $E \, d\Omega_0 = e \, d\Omega_t$, we obtain the following correspondance for the left hand side of Eq. (25):

$$\int_{\Omega_t} \frac{d^s e}{dt} + e \operatorname{div} \mathbf{v}_s \, d\Omega_t \equiv \frac{d^s}{dt} \int_{\Omega_t} e \, d\Omega_t = \int_{\Omega_0} \dot{E} \, d\Omega_0 \quad (27)$$

Likewise, for the terms on the right-hand side, we have

$$\int_{\Omega_t} \boldsymbol{\sigma} : \nabla_{\mathbf{x}} \mathbf{v}_s \, d\Omega_t = \int_{\Omega_0} \mathbf{P} : \dot{\mathbf{F}} \, d\Omega_0 \quad (28)$$

where $\mathbf{P} = J\boldsymbol{\sigma}\mathbf{F}^{-T}$ is the total first Piola-Kirchhoff stress tensor,

$$\int_{\Omega_t} \operatorname{div} \mathbf{q} \, d\Omega_t = \int_{\Omega_0} \operatorname{Div} \mathbf{Q} \, d\Omega_0 \quad (29)$$

where $\mathbf{Q} = J\mathbf{F}^{-1}\mathbf{q}$ is the material heat flux vector, and so on for the other terms:

$$\begin{aligned} \int_{\Omega_t} \operatorname{div}(h_f \mathbf{q}_f) \, d\Omega_t &= \int_{\Omega_0} \operatorname{Div}(h_f \mathbf{Q}_f) \, d\Omega_0 \\ \int_{\Omega_t} \mathbf{f} \cdot \mathbf{q}_f \, d\Omega_t &= \int_{\Omega_0} \mathbf{f} \cdot \mathbf{F} \mathbf{Q}_f \, d\Omega_0 \\ \int_{\Omega_t} \mathfrak{m} \cdot \frac{d^s \mathfrak{b}}{dt} \, d\Omega_t &= \int_{\Omega_0} -\mathfrak{M} \cdot \mathfrak{B} \mathbf{F}^{-T} : \dot{\mathbf{F}} + \mathbf{F}^{-T} \mathfrak{M} \otimes \mathfrak{B} : \dot{\mathbf{F}} + \mathfrak{M} \cdot \dot{\mathfrak{B}} \, d\Omega_0 \end{aligned} \quad (30)$$

where, for this latter, use has been made of the relations (10)₂ and (10)₃ together with the well known kinematic relation $\dot{\mathbf{J}} = J\mathbf{F}^{-T} : \dot{\mathbf{F}}$.

Hence, the material counterpart of the local form (26) is then

$$\begin{aligned} \dot{E} &= \mathbf{P} : \dot{\mathbf{F}} - \operatorname{Div}(h_f \mathbf{Q}_f) - \operatorname{Div} \mathbf{Q} + \mathbf{f} \cdot \mathbf{F} \mathbf{Q}_f \\ &\quad + \mathfrak{M} \cdot \mathfrak{B} \mathbf{F}^{-T} : \dot{\mathbf{F}} - \mathbf{F}^{-T} \mathfrak{M} \otimes \mathfrak{B} : \dot{\mathbf{F}} - \mathfrak{M} \cdot \dot{\mathfrak{B}} \end{aligned} \quad (31)$$

where one can notice the presence of the three last terms related to the magnetic coupling. The former ones are classical in poromechanics, see e.g. Armero (1999); Coussy (2004).

3.2. Second principle and main dissipation inequality

The second law of thermodynamics postulates the positiveness of the entropy production. It is written in the spatial configuration as

$$\frac{d^s}{dt} \int_{\Omega_t} \rho_s (1-n) s_s \, d\Omega_t + \frac{d^f}{dt} \int_{\Omega_t} \rho_f n s_f \, d\Omega_t \geq - \int_{\partial\Omega_t} \frac{\mathbf{q} \cdot \mathbf{n}}{T} \, da \quad (32)$$

where s_s and s_f are the specific entropies of the skeleton's constitutive matrix and the fluid, respectively, and T is the absolute temperature.

Denoting by S the total entropy per unit reference volume such that $Sd\Omega_0 = [\rho_s(1-n)s_s + \rho_f n s_f]d\Omega_t$, pull-back of the inequality (32) to the reference configuration using similar computations as those for the first principle, Section 3.1, we end up with the local form

$$\mathcal{E} = \dot{S} + \text{Div}\left(s_f \mathbf{Q}_f + \frac{\mathbf{Q}}{T}\right) \geq 0 \quad (33)$$

for the rate of entropy production \mathcal{E} .

Now defining the *volumetric* free energy ψ of the porous material as a whole, and the specific free enthalpy of the fluid alone μ_f , respectively as

$$\psi = E - TS \quad \text{and} \quad \mu_f = h_f - Ts_f \quad (34)$$

we can write the total dissipation $\mathcal{D} = T\mathcal{E}$ as

$$\mathcal{D} = \mathcal{D}_{\text{thr}} + \mathcal{D}_{\text{flw}} + \mathcal{D}_{\text{int}} \geq 0 \quad (35)$$

where

$$\begin{aligned} \mathcal{D}_{\text{thr}} &= -\frac{1}{T} \mathbf{Q} \cdot \nabla_{\mathbf{X}} T \\ \mathcal{D}_{\text{flw}} &= -\mathbf{Q}_f \cdot (\nabla_{\mathbf{X}} \mu_f)_T + \mathbf{f} \cdot \mathbf{F} \mathbf{Q}_f \\ \mathcal{D}_{\text{int}} &= \mathbf{P} : \dot{\mathbf{F}} + \mu_f \dot{M}_f - S \dot{T} \\ &\quad + \mathbb{M} \cdot \mathbb{B} \mathbf{F}^{-T} : \dot{\mathbf{F}} - \mathbf{F}^{-T} \mathbb{M} \otimes \mathbb{B} : \dot{\mathbf{F}} - \mathbb{M} \cdot \dot{\mathbb{B}} - \dot{\psi} \end{aligned} \quad (36)$$

after combining Eqs. (31) and (33), and using the fluid mass conservation, Eq. (6). In Eq. (36)₂, $(\nabla_{\mathbf{X}} \mu_f)_T$ stands for the material gradient of μ_f taken at temperature T held constant.

In the Clausius-Duhem inequality (35), we distinguish three forms of dissipation: \mathcal{D}_{thr} due to the heat conduction, \mathcal{D}_{flw} due to the seepage process, and the internal dissipation \mathcal{D}_{int} in the porous material. These three forms are common in thermo-poromechanics, except for the additional terms in (36)₃ that arise from the contribution to the internal dissipation of the magnetic coupling.

A Fourier-type law for the definition of the heat flux vector \mathbf{q} (or \mathbf{Q}) is sufficient to satisfy $\mathcal{D}_{\text{thr}} \geq 0$. Likewise, for the seepage process, Darcy's law furnishes an example for the definition of the flow vector of fluid mass \mathbf{q}_f (or \mathbf{Q}_f) that satisfies $\mathcal{D}_{\text{flw}} \geq 0$. Now following common arguments in continuum thermodynamics, the non-negative dissipation due to internal processes in the porous material is imposed separately, see e.g. Truesdell and Noll (1965); Germain et al. (1983). Its treatment is detailed in the next section.

3.3. Internal dissipation and constitutive equations

In a first step, we rewrite the expression (36)₃ in a more convenient form. For this, let ψ_{sk} and S_{sk} be the free energy and the entropy of the solid skeleton *alone*, both per unit reference volume, and respectively given by

$$\psi_{sk} = \psi - M_f \psi_f \quad \text{and} \quad S_{sk} = S - M_f s_f \quad (37)$$

where $\psi_f = \mu_f - p/\rho_f$ is the specific free energy of the fluid, *i.e.* after combining (B.7) with (B.9) in Appendix B. That is, ψ_{sk} is obtained by extracting the volumetric free energy of the fluid from the total volumetric free energy ψ and, likewise, S_{sk} is obtained by extracting the volumetric entropy of the fluid from the total volumetric entropy S . Then, with the

help of definition (5) for the fluid mass content and the state laws (B.10) for the fluid, the internal dissipation (36)₃ takes the new form

$$\begin{aligned} \mathcal{D}_{\text{int}} = & \mathbf{P} : \dot{\mathbf{F}} + p \dot{\phi} - S_{sk} \dot{T} \\ & + \mathbb{M} \cdot \mathbb{B} \mathbf{F}^{-T} : \dot{\mathbf{F}} - \mathbf{F}^{-T} \mathbb{M} \otimes \mathbb{B} : \dot{\mathbf{F}} - \mathbb{M} \cdot \dot{\mathbb{B}} - \dot{\psi}_{sk} \end{aligned} \quad (38)$$

where, among others, one can notice the conjugate character between the pore pressure p and the Lagrangian porosity ϕ , instead of the one between μ_f and M_f that appears in (36)₃. However, in this form, ϕ is the independent variable for the fluid part and we wish to use p instead, *i.e.* we want ϕ as a function of p and not the reverse, see e.g. Biot (1972). For this, the free energy ψ_{sk} is partially inverted through the partial Legendre transformation

$$\mathcal{L}_{sk} = \psi_{sk} - p\phi \quad (39)$$

and the internal dissipation becomes then

$$\begin{aligned} \mathcal{D}_{\text{int}} = & \mathbf{P} : \dot{\mathbf{F}} - \phi \dot{p} - S_{sk} \dot{T} \\ & + \mathbb{M} \cdot \mathbb{B} \mathbf{F}^{-T} : \dot{\mathbf{F}} - \mathbf{F}^{-T} \mathbb{M} \otimes \mathbb{B} : \dot{\mathbf{F}} - \mathbb{M} \cdot \dot{\mathbb{B}} - \dot{\mathcal{L}}_{sk} \geq 0 \end{aligned} \quad (40)$$

with a free energy of the general form $\mathcal{L}_{sk} \equiv \mathcal{L}_{sk}(\mathbf{F}, \mathbb{B}, p, T)$. Without loss of generality, material dissipations such as plasticity or viscoelasticity are not considered for the sake of clarity. Using the standard arguments of continuum thermodynamics, see for example Coleman and Gurtin (1967); Germain et al. (1983), we get the following state laws

$$\begin{aligned} \mathbf{P} = \frac{\partial \mathcal{L}_{sk}}{\partial \mathbf{F}} - \mathbb{M} \cdot \mathbb{B} \mathbf{F}^{-T} + \mathbf{F}^{-T} \mathbb{M} \otimes \mathbb{B}, \quad \mathbb{M} = -\frac{\partial \mathcal{L}_{sk}}{\partial \mathbb{B}}, \\ \phi = -\frac{\partial \mathcal{L}_{sk}}{\partial p} \quad \text{and} \quad S_{sk} = -\frac{\partial \mathcal{L}_{sk}}{\partial T}. \end{aligned} \quad (41)$$

To simplify further these constitutive equations, we introduce by similar arguments as in Dorfmann and Ogden (2004a,b) the augmented volumetric free energy Ω_{sk} as

$$\Omega_{sk}(\mathbf{F}, \mathbb{B}, p, T) = \mathcal{L}_{sk}(\mathbf{F}, \mathbb{B}, p, T) + \frac{1}{2}\mu_0^{-1}J^{-1}\mathbf{C}:\mathbb{B} \otimes \mathbb{B} \quad (42)$$

With this latter, the augmented first Piola-Kirchhoff stress tensor $\tilde{\mathbf{P}} \equiv \mathbf{P} + \mathbf{P}_m$ is directly obtained by the simple form

$$\tilde{\mathbf{P}} = \frac{\partial \Omega_{sk}}{\partial \mathbf{F}}, \quad (43)$$

where use has been made of the definition (19) for \mathbf{P}_m . Furthermore, the Lagrangian magnetic field vector \mathbb{H} is directly obtained as

$$\mathbb{H} = \frac{\partial \Omega_{sk}}{\partial \mathbb{B}}, \quad (44)$$

after a combination with (41)₂ and the magnetic relation (11). The forms for the Lagrangian porosity and entropy of the solid skeleton remain unchanged:

$$\phi = -\frac{\partial \Omega_{sk}}{\partial p}, \quad \text{and} \quad S_{sk} = -\frac{\partial \Omega_{sk}}{\partial T}. \quad (45)$$

In summary, given the augmented free energy function Ω_{sk} , the results of the constitutive relations (43)-(45) are replaced into: the mechanical balance equation (18), or (17), the fluid mass conservation equation (6), the Maxwell's magnetic equations (9), or (7), and the transient heat equation if any.

Notice further that the internal dissipation, Eq. (40), can now be equivalently rewritten in a more compact form as

$$\mathcal{D}_{\text{int}} = \tilde{\mathbf{P}}:\dot{\mathbf{F}} - \phi\dot{p} - S_{sk}\dot{T} + \mathbb{H}:\dot{\mathbb{B}} - \dot{\Omega}_{sk} \geq 0 \quad (46)$$

where, among others, the conjugate character between \mathbb{H} and \mathbb{B} replaces the one between \mathbb{M} and \mathbb{B} .

3.4. Formulation based on the magnetic field

If instead of the magnetic induction vector \mathbb{B} , we wish to use the magnetic field vector \mathbb{H} as the main independent magnetic variable, we define then the complementary version of Ω_{sk} , denoted by Ω_{sk}^* , through the following partial Legendre transformation

$$\Omega_{sk}^*(\mathbf{F}, \mathbb{H}, p, T) = \Omega_{sk}(\mathbf{F}, \mathbb{B}, p, T) - \mathbb{H} \cdot \mathbb{B} \quad (47)$$

so that, when replaced into the inequality (46), the following state laws are deduced

$$\tilde{\mathbf{P}} = \frac{\partial \Omega_{sk}^*}{\partial \mathbf{F}}, \quad \mathbb{B} = -\frac{\partial \Omega_{sk}^*}{\partial \mathbb{H}}, \quad \phi = -\frac{\partial \Omega_{sk}^*}{\partial p}, \quad S_{sk} = -\frac{\partial \Omega_{sk}^*}{\partial T}. \quad (48)$$

This very useful correspondance has been established by Bustamante et al. (2006) for a similar formulation developed for closed systems. Now it remains to precise the general form of the function Ω_{sk}^* in Eq. (47). For this, we use the complementary version χ_{sk} of the volumetric free energy \mathcal{L}_{sk} , Eq. (39), that depends this time on the magnetic field \mathbb{H} instead of the magnetic induction \mathbb{B} . It is given by

$$\chi_{sk}(\mathbf{F}, \mathbb{H}, p, T) = \mathcal{L}_{sk}(\mathbf{F}, \mathbb{B}, p, T) + \frac{1}{2} \mu_0 J \mathbf{C}^{-1} : \mathbb{M} \otimes \mathbb{M}, \quad (49)$$

see e.g. Kovetz (2000); Steigmann (2004); Bustamante et al. (2008) for a similar relation written in terms of the spatial magnetic vectors \mathbb{h} , \mathbb{b} and \mathbb{m} . Hence, after combining Eqs. (49) and (42) into Eq. (47), and using the magnetic relation (11), the following form is obtained

$$\Omega_{sk}^*(\mathbf{F}, \mathbb{H}, p, T) = \chi_{sk}(\mathbf{F}, \mathbb{H}, p, T) - \frac{1}{2} \mu_0 J \mathbf{C}^{-1} : \mathbb{H} \otimes \mathbb{H}. \quad (50)$$

In summary for a formulation based on the magnetic field vector, the augmented free energy function Ω_{sk}^* has the form (50) and is used for the constitutive relations given in (48). These latter are replaced as usual into the mechanical balance equation (18), or (17), the fluid mass conservation equation (6), the Maxwell's magnetic equations (9), or (7), and the transient heat equation if any.

4. Modeling hyperelastic magneto-active foams

Of interest for the developments presented below is the consideration of porous materials with fully reversible deformations. One can think to the example of macroporous ferrogels that change drastically their porosity and volume in response to the application of external magnetic fields, see for example Zhao et al. (2011); Hong et al. (2014). These materials are isotropic and, for the sake of simplicity, it is further assumed here that the temperature is constant. We choose to consider the magnetic field vector \mathbb{H} as the main independent magnetic quantity and we leave the magnetic induction vector \mathbb{B} to be determined using a constitutive law. We therefore use the augmented free energy function Ω_{sk}^* introduced earlier in Section 3.4.

Now for objectivity reasons, the free energy function χ_{sk} in Eq. (50) must depend on the deformation gradient \mathbf{F} only through the right Cauchy-Green tensor \mathbf{C} , and for symmetry reasons, it depends on the magnetic field vector \mathbb{H} only through the tensor product $\mathbb{H} \otimes \mathbb{H}$, *i.e.* $\chi_{sk} \equiv \chi_{sk}(\mathbf{C}, \mathbb{H} \otimes \mathbb{H}, p)$. Then, use of the property

$$\frac{\partial \Omega_{sk}^*}{\partial \mathbf{F}} = 2\mathbf{F} \frac{\partial \Omega_{sk}^*}{\partial \mathbf{C}}$$

gives the equivalent form for the state laws in (48):

$$\tilde{\boldsymbol{\tau}} \equiv J\tilde{\boldsymbol{\sigma}} = \mathbf{F} \underbrace{2 \frac{\partial \Omega_{sk}^*}{\partial \mathbf{C}}}_{\tilde{\mathbf{S}}} \mathbf{F}^T, \quad J\mathbb{b} = -\mathbf{F} \frac{\partial \Omega_{sk}^*}{\partial \mathbb{H}}, \quad \phi \equiv Jn = -\frac{\partial \Omega_{sk}^*}{\partial p} \quad (51)$$

where we have defined the augmented Kirchhoff stress tensor $\tilde{\boldsymbol{\tau}}$. Furthermore, being an isotropic function of its arguments, χ_{sk} depends in the most general case on the collection of six irreducible invariants, see for example Spencer (1984); Holzapfel (2000); Steigmann (2004) for more details,

$$\begin{aligned} I_1 &= \mathbf{C} : \mathbf{1}, & I_2 &= \frac{1}{2} (I_1^2 - \mathbf{C} : \mathbf{C}), & I_3 &= \det \mathbf{C} \equiv J^2, \\ I_4 &= \mathbb{H} \cdot \mathbb{H}, & I_5 &= \mathbf{C} : \mathbb{H} \otimes \mathbb{H}, & \text{and} & I_6 &= \mathbf{C}^2 : \mathbb{H} \otimes \mathbb{H}, \end{aligned} \quad (52)$$

where the first three ones are classical in isotropic hyperelasticity, and the latter three ones, the so called pseudo-invariants, arise from the coupling with magnetics.

To make matters as concrete as possible, the following augmented volumetric free energy that conforms with the general form (50) will be adopted in our modeling:

$$\Omega_{sk}^* = \underbrace{\chi'_{sk}(\mathbf{C}) + \chi_{por}(J, p)}_{\text{poromechanics}} + \underbrace{c_1 I_4 + c_2 I_5 + c_3 I_6}_{\text{magnetic coupling}} - \underbrace{\frac{1}{2} \mu_0 J \mathbf{C}^{-1} : \mathbb{H} \otimes \mathbb{H}}_{\text{augmentation}} \quad (53)$$

where c_1 , c_2 and c_3 are material parameters. The first two terms are related to the purely poromechanic part of the response, see for example Nedjar (2013a, 2014): χ'_{sk} characterizes the drained response of the solid skeleton without the porous space contribution. It depends at most on the above three invariants I_1 , I_2 and I_3 . The function χ_{por} is the part that accounts for the action of the pore pressure on the solid skeleton through the internal walls of

the porous space. Its dependence on the deformation gradient only through its Jacobian J is clear since, by essence, it is a volumetric phenomenon. Here and in all what follows, the prime notation $(\bullet)'$ refers to effective drained quantities, and not a derivative with respect to any of their arguments.

Hence, the augmented stress tensor of the second Piola-Kirchhoff type, Eq. (51)₁, is given by

$$\begin{aligned} \tilde{\mathbf{S}} = \mathbf{S}' + \mathbf{S}_{por} &+ 2c_2 \mathbb{H} \otimes \mathbb{H} + 2c_3 \{ \mathbb{H} \otimes \mathbb{H}\mathbf{C} + \mathbf{C}\mathbb{H} \otimes \mathbb{H} \} \\ &- \frac{1}{2} \mu_0 J (\mathbf{C}^{-1} : \mathbb{H} \otimes \mathbb{H}) \mathbf{C}^{-1} + \mu_0 J \mathbf{C}^{-1} \mathbb{H} \otimes \mathbb{H} \mathbf{C}^{-1} \end{aligned} \quad (54)$$

with, for the purely poromechanics part $\mathbf{S} = \mathbf{S}' + \mathbf{S}_{por}$

$$\mathbf{S}' = 2 \frac{\partial \chi'_{sk}}{\partial \mathbf{C}} \quad \text{and} \quad \mathbf{S}_{por} = J \mathbf{C}^{-1} \frac{\partial \chi_{por}}{\partial J} \quad (55)$$

where, among others, use has been made of the well known kinematic formula $\partial J / \partial \mathbf{C} = \frac{1}{2} J \mathbf{C}^{-1}$. Equivalently for the Kirchhoff type stress tensor, we have

$$\begin{aligned} \tilde{\boldsymbol{\tau}} = \boldsymbol{\tau}' + \boldsymbol{\tau}_{por} &+ 2c_2 \mathbf{b} \mathbb{h} \otimes \mathbb{h} \mathbf{b} + 2c_3 \{ \mathbf{b} \mathbb{h} \otimes \mathbb{h} \mathbf{b}^2 + \mathbf{b}^2 \mathbb{h} \otimes \mathbb{h} \mathbf{b} \} \\ &- \frac{1}{2} \mu_0 J \mathbb{h} \cdot \mathbb{h} \mathbf{1} + \mu_0 J \mathbb{h} \otimes \mathbb{h} \end{aligned} \quad (56)$$

where $\mathbf{b} = \mathbf{F} \mathbf{F}^T$ is the (spatial) left Cauchy-Green tensor, and where we have used the relation (10)₁ for \mathbb{h} . For the poromechanics part $\boldsymbol{\tau} = \boldsymbol{\tau}' + \boldsymbol{\tau}_{por}$, we have

$$\boldsymbol{\tau}' = \mathbf{F} \mathbf{S}' \mathbf{F}^T \equiv 2 \frac{\partial \chi'_{sk}}{\partial \mathbf{b}} \mathbf{b} \quad \text{and} \quad \boldsymbol{\tau}_{por} = J \frac{\partial \chi_{por}}{\partial J} \mathbf{1} \quad (57)$$

where, for (57)₁, use has been made of the well known result in isotropic elasticity since the three invariants of \mathbf{b} are the same as the above ones I_1 , I_2 and I_3 for \mathbf{C} , see e.g. Truesdell and Noll (1965); Chadwick (1976); Marsden and Hughes (1983). Furthermore, observe from (57)₂ the spherical character

of the Cauchy stress tensor $\boldsymbol{\sigma}_{por} = J^{-1}\boldsymbol{\tau}_{por}$ due to the presence of the internal fluid pore pressure.

For the magnetic induction vector, we have from Eqs. (53) and (48)₂,

$$\begin{aligned}\mathbb{B} &= \underbrace{-2c_1\mathbb{H} - 2c_2\mathbf{C}\mathbb{H} - 2c_3\mathbf{C}^2\mathbb{H}}_{=\mu_0 J\mathbf{C}^{-1}\mathbb{M}} + \mu_0 J\mathbf{C}^{-1}\mathbb{H} \\ &= \mu_0 J\mathbf{C}^{-1}\mathbb{M}\end{aligned}\quad (58)$$

or equivalently for the Kirchhoff-like spatial version, Eq. (51)₂,

$$\begin{aligned}J\mathbb{b} &= \underbrace{-2c_1\mathbf{b}\mathbb{h} - 2c_2\mathbf{b}^2\mathbb{h} - 2c_3\mathbf{b}^3\mathbb{h}}_{=\mu_0 J\mathbb{m}} + \mu_0 J\mathbb{h} \\ &= \mu_0 J\mathbb{m}\end{aligned}\quad (59)$$

which, when compared with the relations (11) and (8), respectively, one concludes that the parameters c_1 , c_2 and c_3 are in fact the magnetization parameters.

For the porosity, the state law (48)₃, or (51)₃, gives

$$\phi \equiv Jn = -\frac{\partial\chi_{por}}{\partial p}\quad (60)$$

This latter will be particularly detailed in the following section.

4.1. Porosity law

The magneto-active porous materials are in general characterized by a high porosity that can drastically change under the action of mechanical forces and/or magnetic fields. The porosity law must then be able to describe this fact, but always keeping in mind that the (true) Eulerian porosity n is by definition a volume fraction and, by consequence, is restricted to always belong to the interval $[0, 1]$. Among the laws proposed in Nedjar (2013a) that satisfy this restriction, we choose here the following simplified one

$$n \equiv n(J, p) = 1 - (1 - h(J)) \exp\left[-\frac{p - p_0}{(1 - f_0)Q}\right]\quad (61)$$

where p_0 is the initial pore pressure, f_0 is the initial connected porosity, Q is a Biot-like modulus, and the function $h(J)$ is defined as

$$h(J) = \begin{cases} f_0 J^m & \text{for } J \leq 1 \\ 1 - (1 - f_0) \exp \left[-\frac{f_0 m}{1 - f_0} (J - 1) \right] & \text{for } J \geq 1 \end{cases} \quad (62)$$

where $m > 0$ is a material parameter. This latter function is no more than the *drained* porosity law since $h(J) \equiv n(J, p = p_0)$. Observe further that, see Figure 2 for an illustration:

- For a high pore pressure, the actual porosity is limited by the upper physical bound, $n \rightarrow 1^-$.
- Under drained conditions with $p = p_0$, the porosity *strictly* belongs to the interval $[0, 1]$.
- At the limiting case of an infinitesimal theory with $J \approx 1 + \varepsilon$, where $\varepsilon \ll 1$ is the infinitesimal volumetric strain, a first order development of the expression (61) near $p = p_0$ gives the relation

$$n = f_0 + f_0 m \varepsilon + \frac{p - p_0}{Q}$$

which is the classical Biot's linear porosity law interpreting the above parameter Q as the initial Biot's modulus, and the product $f_0 m \equiv b$ as the so-called Biot's coefficient, e.g. see Biot (1941); Coussy (2004).

The partial volumetric free energy function $\chi_{por}(J, p)$ that leads to the porosity law (61) through the state law (60) and satisfies the requirements

$$\chi_{por}(J = 1, p = p_0) = 0 \quad \text{and} \quad \frac{\partial \chi_{por}}{\partial J}(J, p = p_0) = 0.$$

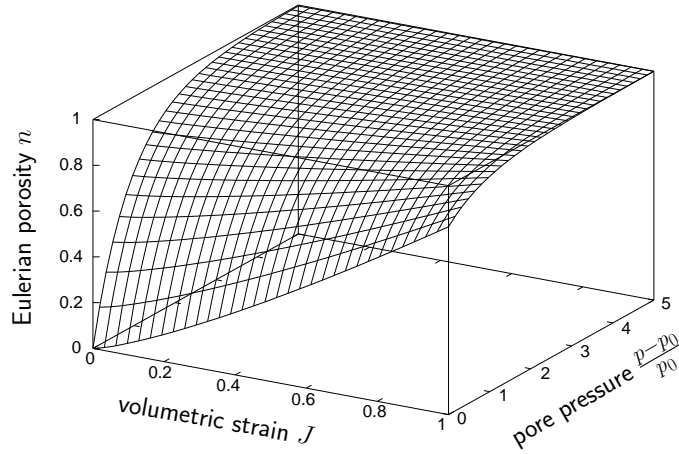


Figure 2: Porosity law $n(J, p)$. An illustration for $J \leq 1$ and $p \geq p_0$.

is given by

$$\chi_{por} = -J(p - p_0) - J(1 - h(J))Q(1 - f_0) \left(\exp \left[-\frac{p - p_0}{Q(1 - f_0)} \right] - 1 \right) \quad (63)$$

With this latter, the stress part due to the action of the internal pore pressure on the solid skeleton is defined as well, *i.e.* Eq. (55)₂ for \mathbf{S}_{por} , or Eq. (57)₂ for $\boldsymbol{\tau}_{por}$.

4.2. Variational formulation of the coupled problem

In magnetostatics, the magnetic field vector can be expressed as the gradient of some magnetic scalar potential that we denote here by φ , see for example Steigmann (2004) for more details. We write

$$\mathbb{H} = -\nabla_{\mathbf{X}}\varphi \quad \Leftrightarrow \quad \mathbf{h} = -\nabla_{\mathbf{x}}\varphi \quad (64)$$

so that the Ampère's equation (7)₁, or (9)₁, is identically satisfied. It remains then to solve the Gauss's equation (7)₂, or (9)₂.

The balance equations consist then of a system involving the mechanical equilibrium, the magnetic Gauss's equation, and the fluid mass conservation. In a finite domain of the reference configuration Ω_0 , the weak form of the three-field coupled problem at hand is:

$$\begin{aligned}
\int_{\Omega_0} \tilde{\mathbf{P}} : \nabla_{\mathbf{X}}(\delta \mathbf{u}) \, d\Omega_0 &= G^{\text{ext}}(\delta \mathbf{u}) \\
\int_{\Omega_0} \mathbb{B} \cdot \nabla_{\mathbf{X}}(\delta \varphi) \, d\Omega_0 &= \int_{\partial\Omega_0} \delta \varphi \bar{Q} \, dA \\
\int_{\Omega_0} \delta p \dot{M}_f - \mathbf{Q}_f \cdot \nabla_{\mathbf{X}}(\delta p) \, d\Omega_0 &= 0
\end{aligned} \tag{65}$$

which must hold for any admissible variations $\delta \mathbf{u}$, $\delta \varphi$ and δp , of displacement, magnetic potential and pore pressure, respectively. Eq. (65)₁ is equivalent to the strong form (18) where $G^{\text{ext}}(\delta \mathbf{u})$ is a short hand notation for the virtual work of external mechanical loading, assumed for simplicity to be deformation independent.

Eq. (65)₂ is the weak form of Gauss's equation (9)₂ where $\bar{Q} = \mathbb{B} \cdot \mathbf{N}$ is the eventual nominal magnetic induction imposed on the boundary $\partial\Omega_0$ of unit normal \mathbf{N} , or on part of it. Notice here that, for the sake of simplicity, the effect of the surrounding space is not considered regarding the magnetic field which normally must be satisfied everywhere, and not only inside the body. So that, Eq. (65)₂ is in fact an approximation.

Finally, Eq. (65)₃ is equivalent to the strong form (6) with the pore pressure field p as primary variable. For simplicity, only Dirichlet-type boundary conditions are considered in the presentation for this latter. Darcy's law is used for the filtration vector $\boldsymbol{\nu}$, see Eq. (4), so that the spatial flow vector of

fluid mass is defined as well:

$$\boldsymbol{\nu} = -k\nabla_{\mathbf{x}}p \quad \Rightarrow \quad \mathbf{q}_f = -\rho_f k\nabla_{\mathbf{x}}p \quad (66)$$

where the gravity effects are neglected. The parameter $k > 0$ is the spatial permeability coefficient of the isotropic porous medium and, by the Piola transform, the material flow vector \mathbf{Q}_f in Eq. (65)₃ is then given by

$$\mathbf{Q}_f = -\rho_f Jk\mathbf{C}^{-1}\nabla_{\mathbf{X}}p \quad (67)$$

where the useful relation $\nabla_{\mathbf{x}}(\cdot) = \mathbf{F}^{-T}\nabla_{\mathbf{X}}(\cdot)$, for scalar fields, has been used.

Last but not least, and irrespective of the solid skeleton, the actual density of the saturating fluid must be linked to the pore pressure p by specifying a constitutive law. The fluid being considered here as barotropic, $\rho_f \equiv \rho_f(p)$, we use the polytropic-like law proposed in Nedjar (2013a),

$$\rho_f(p) = \rho_{f_0} \left(\frac{p}{p_0} \right)^g \quad (68)$$

where ρ_{f_0} is the initial fluid density, and $g \in [0, 1]$ is a fluid parameter. This law encompasses both ideal gas and incompressible fluids as particular cases under isothermal conditions. In fact, one can immediately notice that:

- for $g = 0$, the fluid is incompressible with $\rho_f(p) = \rho_{f_0}, \forall p$.
- for $g = 1$, the constitutive law reduces to the one for ideal gas.

4.3. *Outlines of the algorithmic approximation*

Different numerical strategies can be employed to solve this strongly coupled problem. One can think of a staggered scheme consisting of an initial solid phase at fixed magnetic potential and fluid content, followed by the

Gauss's equation and the fluid mass conservation, both at fixed deformation, see Nedjar (2014) for a similar development in poromechanics. However, as a first attempt, we choose here to use a high fidelity solution procedure by using a *monolithic* scheme where the three sub-problems are solved simultaneously via an iterative resolution procedure of the Newton-Raphson type. Nevertheless, each of these sub-problems need to be linearized first. Below are the relevant points of this procedure.

4.3.1. Mechanical balance equation

Within a typical time interval $[t_n, t_{n+1}]$, the displacement \mathbf{u} , the magnetic potential φ , and the pore pressure field p are assumed to be known fields at time t_n , *i.e.* $\{\mathbf{u}_n, \varphi_n, p_n\}$.

Now by noticing the identity $\tilde{\mathbf{P}} : \nabla_{\mathbf{X}}(\delta\mathbf{u}) = \tilde{\boldsymbol{\tau}} : \nabla_{\mathbf{x}}(\delta\mathbf{u})$, Eq. (65)₁ is then linearized as

$$\begin{aligned}
& \int_{\Omega_0} [\nabla_{\mathbf{x}}(\Delta\mathbf{u})\tilde{\boldsymbol{\tau}} \cdot \nabla_{\mathbf{x}}(\delta\mathbf{u}) + \nabla_{\mathbf{x}}^s(\delta\mathbf{u}) : \tilde{\mathbf{C}} : \nabla_{\mathbf{x}}^s(\Delta\mathbf{u})] \, d\Omega_0 \\
& + \int_{\Omega_0} \nabla_{\mathbf{x}}^s(\delta\mathbf{u}) : [-4c_2 \mathbf{b} \nabla_{\mathbf{x}}(\Delta\varphi) \otimes \mathbf{h} \mathbf{b}]^s \, d\Omega_0 \\
& + \int_{\Omega_0} \nabla_{\mathbf{x}}^s(\delta\mathbf{u}) : [-4c_3 \mathbf{b} \nabla_{\mathbf{x}}(\Delta\varphi) \otimes \mathbf{h} \mathbf{b}^2]^s \, d\Omega_0 \\
& + \int_{\Omega_0} \nabla_{\mathbf{x}}^s(\delta\mathbf{u}) : [-4c_3 \mathbf{b}^2 \nabla_{\mathbf{x}}(\Delta\varphi) \otimes \mathbf{h} \mathbf{b}]^s \, d\Omega_0 \tag{69} \\
& + \int_{\Omega_0} \nabla_{\mathbf{x}}^s(\delta\mathbf{u}) : [\mu_0 J \mathbf{h} \cdot \nabla_{\mathbf{x}}(\Delta\varphi) \mathbf{1}] \, d\Omega_0 \\
& + \int_{\Omega_0} \nabla_{\mathbf{x}}^s(\delta\mathbf{u}) : [-2\mu_0 J \nabla_{\mathbf{x}}(\Delta\varphi) \otimes \mathbf{h}]^s \, d\Omega_0 \\
& + \int_{\Omega_0} [\nabla_{\mathbf{x}}^s(\delta\mathbf{u}) : \mathbf{1} J \frac{\partial \sigma_{por}}{\partial p} \Delta p] \, d\Omega_0 = G_{n+1}^{\text{ext}}(\delta\mathbf{u}) - \int_{\Omega_0} \nabla_{\mathbf{x}}^s(\delta\mathbf{u}) : \tilde{\boldsymbol{\tau}} \, d\Omega_0
\end{aligned}$$

where $\Delta \mathbf{u}$, $\Delta \varphi$ and Δp are increments of displacement, magnetic potential, and pore pressure fields, respectively. The first integral of the left hand side represents the classical term composed by the geometric and the material contributions to the linearization, $\tilde{\mathbf{C}}$ being the *augmented* spatial tangent modulus at fixed magnetic potential and pore pressure that is detailed in Appendix C. The last integral of the left hand side represents the solid-fluid coupling term where we have introduced the notation $\sigma_{por} = \partial \chi_{por} / \partial J$ for the volumetric Cauchy stress due to the pore pressure, see Eq. (57)₂. All the intermediate integrals represent the magneto-mechanics coupling, and the right hand side represents the residual of the mechanical part. The notation $(\cdot)^s$ used in Eq. (69) stands for the symmetric part of a second-order tensor. In particular, $\nabla_{\mathbf{x}}^s(\cdot)$ is the symmetric gradient operator.

We have omitted the subscripts $n+1$ for the sake of clarity. Nevertheless, unless otherwise specified, all the variables are understood to be evaluated at the actual time t_{n+1} , *i.e.* $\mathbf{b} \equiv \mathbf{b}_{n+1}$, $\mathfrak{h} \equiv \mathfrak{h}_{n+1}$, $n \equiv n_{n+1} \dots$

4.3.2. Gauss's magnetic equation

For Gauss's equation, by noticing the useful identities

$$\underbrace{\mathbb{B} \cdot \nabla_{\mathbf{x}}(\delta \varphi)}_{= \mathbf{F} \mathbb{B} \cdot \nabla_{\mathbf{x}}(\delta \varphi) \equiv J \mathbf{b} \cdot \nabla_{\mathbf{x}}(\delta \varphi)} - \left(\frac{\partial \Omega_{sk}^*}{\partial \mathbb{H}} \right) \cdot (-\delta \mathbb{H})$$

the linearization of Eq. (65)₂ is then given by

$$\begin{aligned}
& \int_{\Omega_0} \nabla_{\mathbf{x}}(\delta\varphi) \cdot \{ -4c_2 \mathbf{b} \nabla_{\mathbf{x}}^s(\Delta \mathbf{u}) \mathbf{b} \mathbf{h} - 8c_3 [\mathbf{b} \nabla_{\mathbf{x}}^s(\Delta \mathbf{u}) \mathbf{b}^2]^s \mathbf{h} \} \\
& + \nabla_{\mathbf{x}}(\delta\varphi) \cdot \{ \mu_0 J(\nabla_{\mathbf{x}}^s(\Delta \mathbf{u}) : \mathbf{1}) \mathbf{h} - 2\mu_0 J \nabla_{\mathbf{x}}^s(\Delta \mathbf{u}) \mathbf{h} \} \\
& + \nabla_{\mathbf{x}}(\delta\varphi) \cdot \{ 2c_1 \mathbf{b} + 2c_2 \mathbf{b}^2 + 2c_3 \mathbf{b}^3 - \mu_0 J \mathbf{1} \} \nabla_{\mathbf{x}}(\Delta\varphi) \, d\Omega_0 \\
& = \int_{\partial\Omega_0} \delta\varphi \bar{Q} \, dA - \int_{\Omega_0} \nabla_{\mathbf{x}}(\delta\varphi) \cdot J \mathbf{b} \, d\Omega_0
\end{aligned} \tag{70}$$

where the first two terms on the left hand side are related to the magneto-mechanics coupling, and the right hand side is the residual of the magnetic Gauss's balance.

4.3.3. Fluid mass conservation equation

The fluid mass conservation (65)₃ needs first to be discretized in time before linearization. For this, the rate form of the fluid mass content is detailed as

$$\dot{M}_f = g\rho_f J n \frac{\dot{p}}{p} + \rho_f n \dot{J} + \rho_f J \frac{\partial n}{\partial J} \dot{J} + \rho_f J \frac{\partial n}{\partial p} \dot{p}$$

after combining the definitions (1) and (5), and using the fluid law, Eq. (68). Then, an implicit backward-Euler scheme applied to the evolution equation (65)₃ gives the following time-discretized form

$$\begin{aligned}
& \int_{\Omega_0} \delta p \frac{\rho_f J}{\Delta t} n \left\{ g \log \left[\frac{p}{p_n} \right] + \log \left[\frac{J}{J_n} \right] \right\} \\
& + \delta p \frac{\rho_f J}{\Delta t} \left\{ \frac{\partial n}{\partial J} (J - J_n) + \frac{\partial n}{\partial p} (p - p_n) \right\} \\
& + \rho_f J \nabla_{\mathbf{x}}(\delta p) \cdot k \nabla_{\mathbf{x}} p \, d\Omega_0 = 0
\end{aligned} \tag{71}$$

where use has been made of the Darcy's law, Eq. (66)₂, for the flow vector of fluid mass, and where $\Delta t = t_{n+1} - t_n$ for the time interval.

After lengthy, but straightforward algebraic manipulations and collecting terms, the linearization is given by

$$\begin{aligned}
& \int_{\Omega_0} \delta p \frac{\rho_f J}{\Delta t} \left\{ (J - J_n) \left(\frac{\partial n}{\partial J} + J \frac{\partial^2 n}{\partial J^2} \right) + J \frac{\partial n}{\partial J} \right. \\
& + (p - p_n) \left(\frac{\partial n}{\partial p} + J \frac{\partial^2 n}{\partial p \partial J} \right) + n \\
& \left. \left(\log \left[\frac{J}{J_n} \right] + g \log \left[\frac{p}{p_n} \right] \right) \left(n + J \frac{\partial n}{\partial J} \right) \right\} \mathbf{1} : \nabla_{\mathbf{x}}^s(\Delta \mathbf{u}) \\
& + \rho_f J k \left\{ \nabla_{\mathbf{x}}(\delta p) \cdot \nabla_{\mathbf{x}} p \mathbf{1} - 2 \nabla_{\mathbf{x}}(\delta p) \otimes \nabla_{\mathbf{x}} p \right\} : \nabla_{\mathbf{x}}^s(\Delta \mathbf{u}) \, d\Omega_0 \\
& + \int_{\Omega_0} \delta p \frac{\rho_f J}{\Delta t} \left\{ (J - J_n) \left(\frac{g}{p} \frac{\partial n}{\partial J} + \frac{\partial^2 n}{\partial J \partial p} \right) \right. \\
& + (p - p_n) \left(\frac{g}{p} \frac{\partial n}{\partial p} + \frac{\partial^2 n}{\partial p^2} \right) + \frac{\partial n}{\partial p} + g \frac{n}{p} \\
& \left. \left(\log \left[\frac{J}{J_n} \right] + g \log \left[\frac{p}{p_n} \right] \right) \left(\frac{gn}{p} + \frac{\partial n}{\partial p} \right) \right\} \Delta p \\
& + \rho_f J k \left\{ \nabla_{\mathbf{x}}(\delta p) \cdot \nabla_{\mathbf{x}}(\Delta p) + g \nabla_{\mathbf{x}}(\delta p) \cdot \nabla_{\mathbf{x}} p \frac{\Delta p}{p} \right\} d\Omega_0 = R_f
\end{aligned} \tag{72}$$

where the first integral on the left hand side corresponds to the fluid-solid coupling. R_f is the short hand notation for the residual of the fluid part.

4.3.4. Finite element outlines

In a finite element context, the displacement, the magnetic potential, and the pore pressure fields are defined at the nodes, see Figure 3 for an illustration. The interpolations of the geometry and the three fields are completely standard, see e.g. Hughes (1987); Zienkiewicz and Taylor (2000); Wriggers (2008) for the exposition of these ideas.

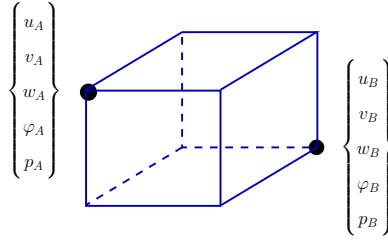


Figure 3: Typical finite element with nodal *dofs* in magneto-poromechanics.

For the monolithic resolution, the element contributions to the *global* tangent stiffness matrix associated with the element nodes are written as

$$\mathbf{K}_e^{AB} = \begin{bmatrix} \mathbf{K}_{e11}^{AB} & \mathbf{K}_{e12}^{AB} & \mathbf{K}_{e13}^{AB} \\ \mathbf{K}_{e21}^{AB} & \mathbf{K}_{e22}^{AB} & 0 \\ \mathbf{K}_{e31}^{AB} & 0 & \mathbf{K}_{e33}^{AB} \end{bmatrix} \in \mathbb{R}^{(n_{\text{dim}}+2) \times (n_{\text{dim}}+2)} \quad (73)$$

for $A, B = 1, \dots, n_{\text{node}}^e$, where n_{node}^e is the number of nodes. In this matrix, the first column (row) is associated with the n_{dim} components of the nodal displacements, the second column (row) is associated with the nodal magnetic potential, and the third column (row) is associated with the nodal fluid pore pressure. The fact that there is no coupling between magnetostatics and fluid mass conservation appears through the vanishing (2,3) terms, *i.e.* $K_{e23}^{AB} = 0$ and $K_{e32}^{AB} = 0$. The expressions of the different sub-matrices are easily deduced from the above linearizations, Eqs. (69), (70) and (72). In particular, the (1,2) terms are symmetric, $K_{e21}^{AB} = (K_{e12}^{AB})^T$, but the (1,3) ones are not. This renders the global tangent matrix non-symmetric.

5. Numerical simulations

Since the solid skeleton is macroscopically compressible, it is beneficial to split the deformation locally into a volumetric part, that depends on the

Jacobian J , and an isochoric part that depends on the modified deformation gradient $J^{-1/3}\mathbf{F}$, as originally proposed by Flory (1961), and successfully applied later on in finite strain elasticity, e.g. see Lubliner (1985); Ogden (1997); Simo and Hughes (1998); Holzapfel (2000) among many others. In practice, any of the existing compressible hyperelastic models proposed in the literature can be used for the effective drained response of the solid skeleton. We choose here a Neo-Hookean type with a free energy given by

$$\chi'_{sk}(\mathbf{C}) = \frac{3}{8}\kappa_{sk} (J^{4/3} + 2J^{-2/3} - 3) + \frac{1}{2}\mu_{sk}(J^{-2/3}\mathbf{C}:\mathbf{1} - 3) \quad (74)$$

where the first term is related to the volumetric response with κ_{sk} as a bulk modulus, and the second term is related to the volume-preserving part of the response with μ_{sk} as a shear modulus. Hence, together with the expression already given for the porous space contribution, $\chi_{por}(J, p)$ in Eq. (63), the augmented free energy (53) is completely defined.

Of interest in this section is the qualitative modeling of macroporous ferrogels that can be used as active porous scaffolds capable of delivering biological agents under the controls of external magnetic stimuli. Various macroporous ferrogels were developed and studied in Zhao et al. (2011). In particular, we consider here the one fabricated with 13 wt % Fe_3O_4 and 1 wt % alginate cross-linked by 5 mM AAD (adipic acid dihydrazide), and frozen at $-20^\circ C$. It is characterized by its highly interconnected (*initial*) porosity, about 82%, and a low initial modulus, about 2.5 *kPa*. We keep in mind these two important informations for the following simulations.

5.1. Response to mechanical loadings

Figure 4 shows the results of compression tests on a cylindrical sample of radius 5 mm and 15 mm height. The lateral free surface is supposed to allow drainage while the top and bottom faces are assumed smooth and impervious. The initial pore pressure is set to $p_0 = 1\text{ atm}$, this latter being the prescribed value of the pore pressure on the lateral surface as a boundary condition for the fluid part. The mechanical loading consists on imposing a displacement on the top face while the bottom one remains fixed. For symmetry reasons, one fourth of the cylinder is considered during the computations.

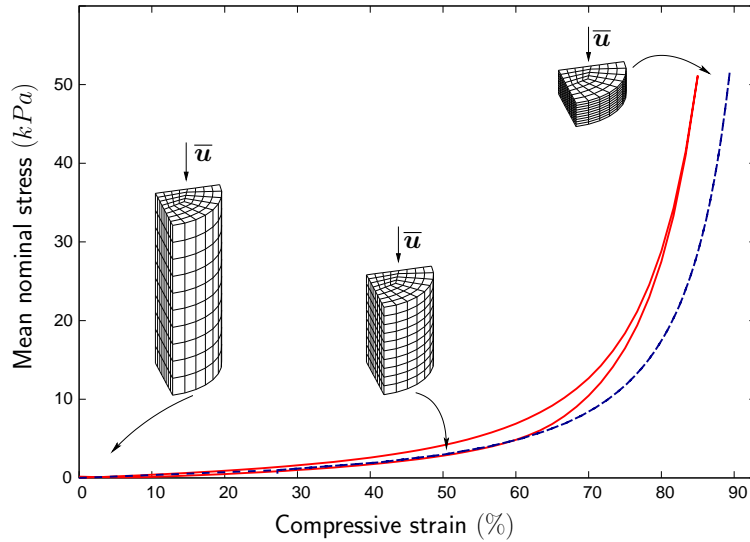


Figure 4: Compression tests on the macroporous ferrogel. Fast loading/unloading at 0.85 s^{-1} (solid curve), and very slow loading/unloading (dashed curve). Finite element mesh and selected deformed configurations at 50% and 85% compressive strains.

The following poromechanics material parameters have been used:

$$\begin{aligned}\kappa_{sk} &= 0.83334 \text{ kPa}, & \mu_{sk} &= 1.25 \text{ kPa}, \\ f_0 &= 0.82, & m &= 1.2, & Q &= 500 \text{ kPa}, \\ k_0 &= 100 \text{ mm}^2/\text{MPa s}, & \rho_{f_0} &= 1.204 \text{ kg/m}^3, & g &= 1\end{aligned}\tag{75}$$

where κ_{sk} and μ_{sk} are such that the Young's modulus is $E_0 = 2.5 \text{ kPa}$ in the limiting case of a linearized kinematics with a zero Poisson's ratio, *i.e.* the macroporous ferrogel behaves like a sponge, see also Hong et al. (2014). Besides on the known initial porosity f_0 , see above, the parameters Q and m are only qualitative. Nevertheless, these (f_0, m, Q) parameters together with $p_0 = 1 \text{ atm}$ are the ones with which the porosity law of Figure 2 has been plotted. For the fluid constitutive law, see Eq. (68), the fluid parameter g corresponds to an ideal gas, ρ_{f_0} being here the initial air density. Finally, the material permeability coefficient k_0 is also qualitative at this stage. Anyhow, this latter influences the rate-effects of the sample's response through Darcy's law. This is shown by comparing the two loading/unloading curves of Figure 4. The dashed one corresponds to the case of a very slow velocity with full drainage, *i.e.* the effective hyperelastic response of the solid skeleton alone. The solid curve corresponds to a faster velocity where the sample is strain compressed at 85% in one second of time. A relative stiffening is observed in this case with the characteristic hysteresis due to the delay caused by the fluid flow during unloading.

Globally, these results are in good agreement with the ones obtained experimentally in (Zhao et al., 2011). The high deformability of the macroporous ferrogel is well captured by the purely poromechanical part of the present modeling framework.

5.2. Macroporous ferrogel under magnetic loading

In this second step, the deformation of macroporous ferrogel under the influence of a magnetic field is examined. The sample we consider is again the above cylinder with the same compressible Neo-Hookean-like material. For the magnetic field, we recall that $\mu_0 = 4\pi 10^{-7} N/A^2$ for the magnetic permeability of vacuum. The magnetization parameters c_1 , c_2 and c_3 , see Eq. (53), would have to be determined experimentally. However, due to the lack of experimental results, material properties are inadequate at this point. Therefore, for the purpose of testing the robustness of our numerical implementation, we assume the following values in this example:

$$c_1 = 1 N/A^2 \quad c_2 = 1 N/A^2 \quad c_3 = 1 N/A^2 \quad (76)$$

to activate the three pseudo-invariants relative to the magnetic coupling in the constitutive relations, see the expressions (54), or (56), for the stress tensor, and (58), or (59), for the magnetic induction vector.

A magnetic potential φ is imposed on the two ends of the cylinder at φ_- and φ_+ , respectively, which create a potential difference $\Delta\varphi = \varphi_+ - \varphi_-$. During the computation, this difference is increased from 0 to 2 A in 20 steps at a loading velocity of 0.5 A/s, and then decreased from 2 to 0 A in 20 steps as well at an unloading velocity of $-0.5 A/s$. For the rest of the boundary conditions, the two end faces are free and impervious, and the lateral surface is free with a prescribed pore pressure set to p_0 for the fluid part. This latter is also the initial pore pressure in the whole cylinder before the magnetic loading.

The deformation of the cylinder is shown in Figure 5 for the magnetic

potential differences $\Delta\varphi = 1 A$ and $\Delta\varphi = 2 A$ during the loading phase. For illustrative purposes, the Eulerian porosity distribution for the latter and the pore pressure field for the former are also shown. Among others, these fields are not uniform within the cylinder and, due to the relatively high permeability of the porous space together with the small dimensions of the sample, the difference of the pore pressure with the initial one, $p_0 = 10^5 N/m^2$, is small.

One can also observe that the deformation easily reaches large levels, more than 70%. This is highlighted in Figure 6 where we have plotted the evolution of the global compressive strain versus the magnetic loading. The hysteresis that appears during unloading illustrates here again the rate-effects due to the fluid-flow.

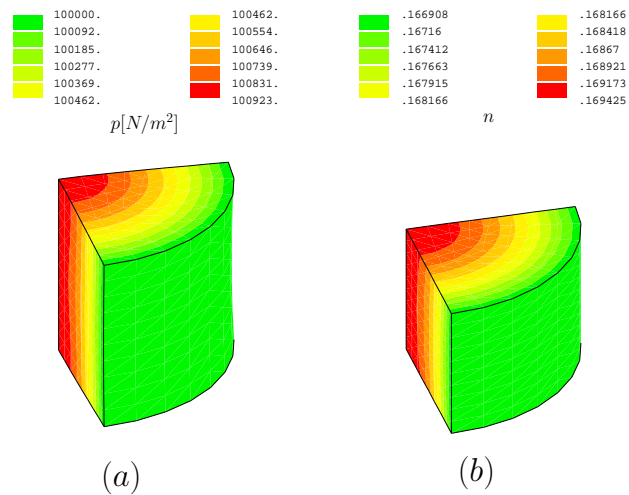


Figure 5: Deformed configuration under: (a) $\Delta\varphi = 1 A$, and (b) $\Delta\varphi = 2 A$.

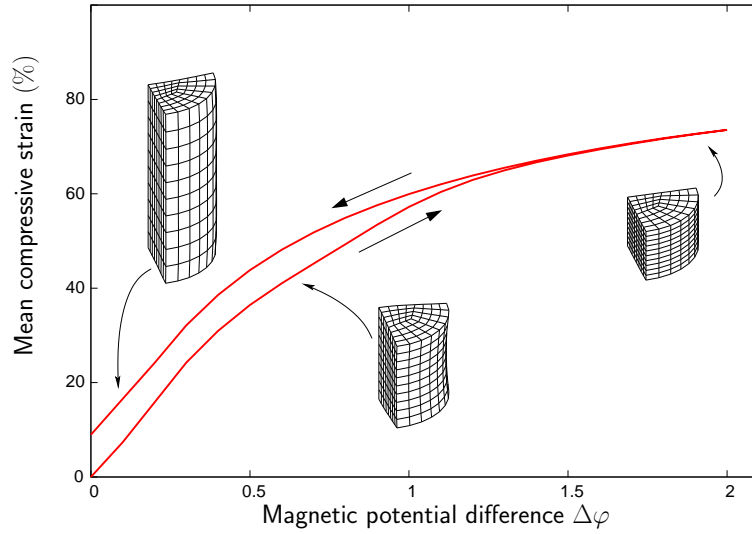


Figure 6: Evolution of the compressive strain with the magnetic loading. Deformed configurations for $\Delta\varphi = 0.6$ and $2 A$ during loading, and $\Delta\varphi = 0.1 A$ during unloading.

5.3. Macroporous ferrogels as active sponges

Macroporous ferrogels can be used as devices in tissue engineering and cell-based therapies to trigger and enhance the release of various biological agents by controlling the external magnetic fields, see Zhao et al. (2011) for more details. It becomes then of major importance to know how the amount of released fluid evolves during the loading history. Within the present theory, this information is provided by the fluid mass conservation equation, *i.e.* by Eq. (6), or equivalently by Eq. (65)₃.

As an example, we consider again the precedent macroporous cylindrical sample of radius 5 mm and 15 mm height. This latter is this time completely submerged in water. The magneto-poromechanics material parameters we use are those given in Eqs. (75)-(76) less those for the fluid's constitutive

law, replaced here by

$$\rho_{f_0} = 1000 \text{ kg/m}^3 \quad \text{and} \quad g = 0$$

for the saturating incompressible water. Initially, the volume of water inside the porous domain is then $\sim 966.04 \text{ mm}^3$ in our case, *i.e.* the initial volume of the cylinder times the initial porosity f_0 .

Now as for the example of Section 5.2, a loading/unloading cycle consists of an increase of the potential difference $\Delta\varphi$ between the end faces from 0 to $2A$ at a velocity of $0.5 A/s$, followed by a decrease from $2A$ to $0A$ at a velocity of $-0.5 A/s$. The boundary conditions are the same as for the precedent example. For illustrative purposes, Figure 7 shows the evolution of the released water volume from the whole cylinder under a one-cycle and a three-cycles magnetic loading histories. Noteworthy observations should be pointed out from these results:

- While the ascending branches of the curves correspond to increasing volume release when the magnetic loading is increasing, the descending ones mean that the released water is being partially reabsorbed with decreasing magnetic loading.
- Once the magnetic loading is off, almost all the released water is reabsorbed after a recovery time and the cylindrical sample returns to its original underformed configuration.
- One can check that, at any time, the computed released volume of water never exceeds the volume that was initially present inside the sample, *i.e.* less than $\sim 966.04 \text{ mm}^3$.

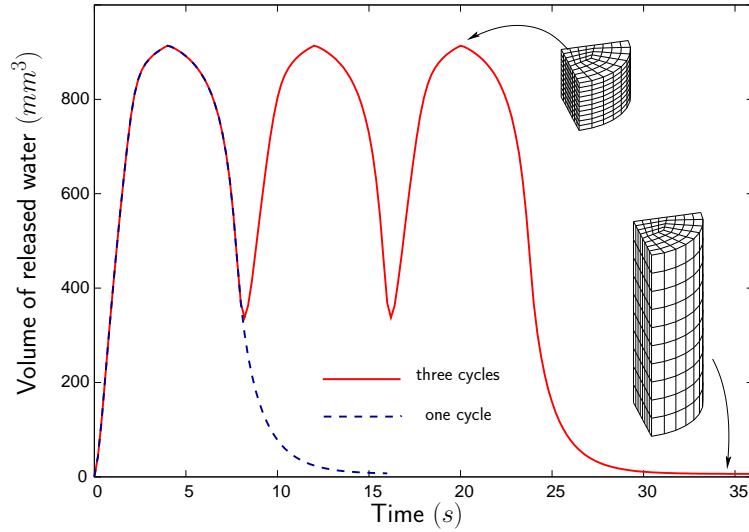


Figure 7: Evolution of the released volume of water from the whole domain under a one-cycle (dashed curve) and a three-cycles (solid curve) magnetic loading histories. The computations are pursued until *almost* total recovery.

6. Conclusion and perspectives

In this paper, we have presented a coupled magneto-poromechanics theory where, for the poromechanics part, use has been made of the macroscale Biot's theory. By means of the continuum thermodynamics of open media, the nowadays well known fields related to the magnetic coupling have been embedded in a sound way for a concise characterization of the whole set of constitutive equations. Furthermore, as large deformation is usually expected due to the soft nature of the materials we have in mind, the present theory has been developed within the finite strain range.

To make matters as concrete as possible, a magneto-hyperelastic model has been presented in detail that can be well adapted for the modeling of

macroporous ferrogels. As these latter can further give high porosity change, a nonlinear porosity law has been used that allows for a good description of the seepage process when the fluid is released and/or reabsorbed. This characteristic can certainly be of particular interest for the design of biomedical devices used to enhance the release of biological agents.

With the finite element method as a tool for structural simulations, the numerical examples presented in this paper have shown an encouragingly good agreement with experimental observations, at least qualitatively. We believe that further work has to be accomplished to optimize the present formulation toward more realistic modeling of smart magneto-active porous materials in general. Experimental investigations will certainly give better knowledge of the material properties. Among others, the correct evaluation of the fluid permeability which, even high and allows rapid recovery, has however a great importance on the seepage process and, consequently, on the rate-depend effects due to the fluid flow. The magnetization parameters c_1 , c_2 and c_3 must be quantified correctly. Experimental tests could for example show which ones are most relevant for the modeling, so that the coupling part of the constitutive relations could then be simplified.

Further algorithmic investigations in conjunction with optimized finite elements are needed. This is especially true for problems where strong distortions at large deformations with highly compressible materials are present. The present global resolution strategy using a simultaneous scheme must be changed in the favor of a staggered scheme exploiting the symmetries of each sub-problem with certainly less computational costs. Moreover, as Maxwell equations must be satisfied not only inside the body, but also in the surround-

ing free space, this fact must be accounted for in future numerical developments. On another hand, when dealing with problems in magnetodynamics, a vector potential formulation must be used together with the magnetic induction vector as main magnetic variable. These points and others will form the substance of separate communications.

Appendix A. Fluid mass conservation within a porous material

Within any volume Ω_t of porous material in the spatial configuration, the Eulerian fluid mass conservation is given by

$$\frac{d^f}{dt} \int_{\Omega_t} \rho_f n \, d\Omega_t = 0 \quad (\text{A.1})$$

where n is the Eulerian porosity and ρ_f is the current fluid density. Eq. (A.1) leads to the following local form:

$$\frac{\partial}{\partial t}(\rho_f n) + \text{div}(\rho_f n \mathbf{v}_f) = 0 \quad (\text{A.2})$$

where \mathbf{v}_f is the velocity of the fluid phase located at \mathbf{x} . Now as the spatial flux vector of fluid mass \mathbf{q}_f is given by, see Figure 1,

$$\mathbf{q}_f = \rho_f n (\mathbf{v}_f - \mathbf{v}_s) \quad (\text{A.3})$$

where \mathbf{v}_s is the velocity of the solid phase at the same location \mathbf{x} , Eq. (A.2) is equivalently rewritten as

$$\frac{d^s}{dt}(\rho_f n) + \rho_f n \text{div} \mathbf{v}_s + \text{div} \mathbf{q}_f = 0 \quad (\text{A.4})$$

in terms of the material time derivative with respect to the solid phase.

Integrating the last result over the actual volume Ω_t gives

$$\frac{d^s}{dt} \int_{\Omega_t} \rho_f n \, d\Omega_t + \int_{\Omega_t} \text{div} \mathbf{q}_f \, d\Omega_t = 0 \quad (\text{A.5})$$

which proves the identity of Eq. (3).

Appendix B. Thermostatistics of fluids

Let us recall basic relations on the thermostatistics of fluids that are useful in the continuum thermodynamic developments of Section 3, see for example Coussy (2004) for more details. The energy conservation reads

$$de_f = -p d\left(\frac{1}{\rho_f}\right) + \delta Q \quad (\text{B.1})$$

where de_f is the change of the specific internal energy of the fluid, δQ is the infinitesimal heat supply, and $-p d(1/\rho_f)$ is the mechanical work supplied to the fluid by the pressure p in the volume change $d(1/\rho_f)$ of its specific volume $1/\rho_f$. Excluding irreversible transformations, the entropy balance reads

$$ds_f = \frac{\delta Q}{T} \quad (\text{B.2})$$

where s_f is the specific entropy of the fluid and T the absolute temperature.

Combination of Eqs. (B.1) and (B.2) by eliminating the heat supply leads to the following energy balance:

$$de_f = -p d\left(\frac{1}{\rho_f}\right) + T ds_f \quad (\text{B.3})$$

This latter means that the specific internal energy has arguments $1/\rho_f$ and s_f , *i.e.* $e_f \equiv e_f(1/\rho_f, s_f)$. By identification, again with Eq. (B.3), we get the state laws

$$p = -\frac{\partial e_f}{\partial\left(\frac{1}{\rho_f}\right)} \quad \text{and} \quad T = \frac{\partial e_f}{\partial s_f} \quad (\text{B.4})$$

- Partial inversion with respect to the pair $(1/\rho_f, p)$ gives the fluid specific enthalpy h_f as

$$h_f \equiv h_f(p, s_f) = e_f - \left(\frac{1}{\rho_f}\right) (-p) = e_f + \frac{p}{\rho_f} \quad (\text{B.5})$$

Hence, the variation of this latter, and use of Eq. (B.3), identify the state laws

$$\frac{1}{\rho_f} = \frac{\partial h_f}{\partial p} \quad \text{and} \quad T = \frac{\partial h_f}{\partial s_f} \quad (\text{B.6})$$

- Partial inversion, this time with respect to the pair (s_f, T) , gives the fluid specific free energy ψ_f as

$$\psi_f \equiv \psi_f\left(\frac{1}{\rho_f}, T\right) = e_f - T s_f \quad (\text{B.7})$$

Its variation together with the use of Eq. (B.3), identify the state laws

$$p = -\frac{\partial \psi_f}{\partial\left(\frac{1}{\rho_f}\right)} \quad \text{and} \quad s_f = -\frac{\partial \psi_f}{\partial T} \quad (\text{B.8})$$

- Finally, total inversion with respect to both pairs gives the fluid specific free enthalpy μ_f , *i.e.* the Gibbs specific potential, as

$$\mu_f \equiv \mu_f(p, T) = e_f + \frac{p}{\rho_f} - T s_f \quad (\text{B.9})$$

with the state laws

$$\frac{1}{\rho_f} = \frac{\partial \mu_f}{\partial p} \quad \text{and} \quad s_f = -\frac{\partial \mu_f}{\partial T} \quad (\text{B.10})$$

Appendix C. Augmented tangent modulus $\tilde{\mathbf{C}}$

As for the augmented stress tensor, Eqs. (54) or (56), the fourth-order tangent modulus $\tilde{\mathbf{C}}$ is given by an additive form as well. We write

$$\tilde{\mathbf{C}} = \mathbf{C}_{sk} + \mathbf{C}_{por} + \mathbf{C}_{mgn} \quad (\text{C.1})$$

where \mathbf{C}_{sk} is the modulus relative to the drained hyperelastic solid skeleton, \mathbf{C}_{por} is the porous space contribution at fixed pore pressure, and \mathbf{C}_{mgn} is

the magnetic contribution at fixed magnetic potential due to both of the magneto-mechanics coupling and the magnetic augmentation.

The derivation of \mathbf{C}_{sk} mimics those for single-phase hyperelastic solids widely developed in the literature, see e.g. Ogden (1997); Simo (1998); Holzapfel (2000); Nedjar (2002a,b, 2011); Wriggers (2008). Details of this nowadays standard notion are skipped here.

For the derivation of the modulus \mathbf{C}_{por} , one proceeds in two steps starting from the definition of the partial state law $\mathbf{S}_{por} = J\sigma_{por}\mathbf{C}^{-1}$, Eq. (55)₂, on the reference configuration where we have defined the (scalar) volumetric Cauchy stress $\sigma_{por} = \partial\chi_{por}/\partial J$:

- *step (i)*: Compute the time derivative such that $\dot{\mathbf{S}}_{por} = \mathbf{\Xi}_{por} : \frac{1}{2}\dot{\mathbf{C}}$, where $\mathbf{\Xi}_{por}$ is the material tangent modulus relative to the porous space.
- *step (ii)*: Then, push-forward of the precedent result to the current configuration with the solid skeleton's deformation gradient \mathbf{F} gives the Lie derivative $\mathcal{L}_v\boldsymbol{\tau}_{por} \equiv \mathbf{F}\dot{\mathbf{S}}_{por}\mathbf{F}^T$ such that $\mathcal{L}_v\boldsymbol{\tau}_{por} = \mathbf{C}_{por} : \mathbf{d}$, where $\mathbf{d} = \text{sym}[\dot{\mathbf{F}}\mathbf{F}^{-1}]$ is the spatial strain rates tensor. The useful kinematic relationship $\dot{\mathbf{C}} = 2\mathbf{F}^T\mathbf{d}\mathbf{F}$ is to be employed during the derivation, see Nedjar (2002, 2007, 2011) for similar developments. The following expression is then obtained

$$\mathbf{C}_{por} = -2J\sigma_{por}\mathbf{I} + J\left\{\sigma_{por} + J\frac{\partial\sigma_{por}}{\partial J}\right\}\mathbf{1} \otimes \mathbf{1} \quad (\text{C.2})$$

The derivation of the modulus \mathbf{C}_{mgn} follows similar lines as for \mathbf{C}_{por} , this

time starting from the partial stress

$$\begin{aligned} \mathbf{S}_{mgn} &= 2c_2 \mathbb{H} \otimes \mathbb{H} + 2c_3 \{ \mathbb{H} \otimes \mathbb{H} \mathbf{C} + \mathbf{C} \mathbb{H} \otimes \mathbb{H} \} \\ &- \frac{1}{2} \mu_0 J \mathbf{C}^{-1} : \mathbb{H} \otimes \mathbb{H} \mathbf{C}^{-1} + \mu_0 J \mathbf{C}^{-1} \mathbb{H} \otimes \mathbb{H} \mathbf{C}^{-1} \end{aligned} \quad (\text{C.3})$$

i.e. the last four terms in Eq. (54). Push-forward of its time derivative to the current configuration, $\mathbf{F} \dot{\mathbf{S}}_{mgn} \mathbf{F}^T$, allows to identify the following partial tangent modulus

$$\begin{aligned} \mathbf{C}_{mgn} &= 4c_3 \mathbf{I}_b + \mu_0 J \mathbb{h} \cdot \mathbb{h} \left\{ \mathbf{I} - \frac{1}{2} \mathbf{1} \otimes \mathbf{1} \right\} \\ &+ \mu_0 J \left\{ \mathbf{1} \otimes \mathbb{h} \otimes \mathbb{h} + \mathbb{h} \otimes \mathbb{h} \otimes \mathbf{1} - 2\mathbf{I}_h \right\} \end{aligned} \quad (\text{C.4})$$

where the fourth-order operators \mathbf{I}_h and \mathbf{I}_b are defined such that:

$$\begin{aligned} \mathbf{I}_h : \mathbf{d} &= \mathbb{h} \otimes \mathbb{h} \mathbf{d} + \mathbf{d} \mathbb{h} \otimes \mathbb{h} \\ \mathbf{I}_b : \mathbf{d} &= (\mathbb{b} \mathbb{h} \otimes \mathbb{h} \mathbb{b}) \mathbf{d} \mathbf{b} + \mathbf{b} \mathbf{d} (\mathbb{b} \mathbb{h} \otimes \mathbb{h} \mathbb{b}). \end{aligned} \quad (\text{C.5})$$

References

- Armero, F., 1999. Formulation and finite element implementation of a multiplicative model of coupled poro-plasticity at finite strains under fully saturated conditions. *Computer Methods in Applied Mechanics and Engineering* **171**, 205–241.
- Baek, S., Pence, T., 2011. Inhomogeneous deformation of elastomer gels in equilibrium under saturated and unsaturated conditions. *Journal of the Mechanics and Physics of Solids* **59**, 561–582.
- Biot, M., 1941. General theory of three-dimensional consolidation. *Journal of Applied Physics* **12**, 155–164.

- Biot, M., 1972. Theory of finite deformation of porous solids. *Indiana University Mathematical Journal* **21**, 597–620.
- Bowen, R., 1982. Compressible porous media models by use of the theory of mixtures. *International Journal of Engineering Science* **20**, 697–735.
- Brigadnov, I., Dorfmann, A., 2003. Mathematical modeling of magneto-sensitive elastomers. *International Journal of Solids and Structures* **40**, 4659–4674.
- Brown, W., 1966. *Magnetoelastic Interactions*. Springer, Berlin.
- Bustamante, R., Dorfmann, A., Ogden, R., 2006. Universal relations in isotropic nonlinear magnetoelasticity. *The Quarterly Journal of Mechanics and Applied Mathematics* **59**, 435–450.
- Bustamante, R., Dorfmann, A., Ogden, R., 2008. On variational formulations in nonlinear magnetoelastostatics. *Mathematics and Mechanics of Solids* **13**, 725–745.
- Chadwick, P., 1976. *Continuum Mechanics. Concise Theory and Problems*. John Wiley and Sons, Inc., New York, NY.
- Coleman, B., Gurtin, M., 1967. Thermodynamics with internal variables. *Journal of Chemicals and Physics* **47**, 597–613.
- Coussy, O., 2004. *Poromechanics*. John Wiley and Sons Inc., New York.
- Dorfmann, A., Ogden, R., 2004a. Nonlinear magnetoelastic deformations. *Quarterly Journal of Mechanics and Applied Mathematics* **57**, 599–622.

- Dorfmann, A., Ogden, R., 2004b. Nonlinear magnetoelastic deformations of elastomers. *Acta Mechanica* **167**(1-2), 13–28.
- Duda, F., Souza, A., Fried, E., 2010. A theory for species migration in a finitely strained solid with application to polymer network swelling. *Journal of the Mechanics and Physics of Solids* **58**, 515–529.
- Ericksen, J., 2006. A modified theory of magnetic effects in elastic materials. *Mathematics and Mechanics of Solids* **11**, 23–47.
- Flory, P., 1961. Thermodynamic relations for high elastic materials. *Transactions of the Faraday Society* **57**, 829–838.
- Germain, P., Nguyen, Q., Suquet, P., 1983. Continuum thermodynamics. *ASME Journal of Applied Mechanics* **50**, 1010–1021.
- Ginder, J., Clark, S., Schlotter, W., Nichols, M., 2002. Magnetostrictive phenomena in magnetorheological elastomers. *International Journal of Modern Physics B* **16**, 2412–2418.
- Holzappel, G., 2000. *Nonlinear Solid Mechanics. A Continuum Approach for Engineering*. John Wiley and Sons, Ltd, Chichester, West Sussex, UK.
- Hong, S., Jung, Y., Yen, R., Chan, H., Leong, K., Truskey, G., Zhao, X., 2014. Magnetoactive sponges for dynamic control of microfluidic flow patterns in microphysiological systems. *Lab on a Chip* **14**, 514–521.
- Hughes, T., 1987. *The Finite Element Method*. Prentice-Hall, Englewood-Cliffs, NJ.

- Jolly, M., Carlson, J., Muñoz, B., 1996. A model of the behavior of magnetorheological materials. *Smart Materials and Structures* **5**, 607–614.
- Kankanala, S., Triantafyllidis, N., 2004. On finitely strained magnetorheological elastomers. *Journal of the Mechanics and Physics of Solids* **52**, 2869–2908.
- Kovetz, A., 2000. *Electromagnetic Theory*. Oxford University Press, Oxford.
- Lewis, R., Schrefler, B., 1998. *The Finite Element Method in the Static and Dynamic Deformation and Consolidation of Porous Media*. John Wiley and Sons Inc., New York.
- Liu, T., Hu, S., Liu, K., Liu, D., Chen, S., 2006. Preparation and characterization of smart magnetic hydrogels and its use for drug release. *Journal of Magnetism and Magnetic Materials* **304**, e397–e399.
- Lubliner, J., 1985. A model of rubber viscoelasticity. *Mechanics Research Communications* **12**, 93–99.
- Marsden, J., Hughes, T., 1983. *Mathematical Foundations of Elasticity*. Prentice-Hall, Englewood-Cliffs, NJ.
- Nedjar, B., 2002. A theoretical and computational setting for a geometrically nonlinear gradient damage modelling framework. *Computational Mechanics* **30**, 65–80.
- Nedjar, B., 2002a. Frameworks for finite strain viscoelastic-plasticity based on multiplicative decompositions. Part I: continuum formulations. *Computer Methods in Applied Mechanics and Engineering* **191**, 1541–1562.

- Nedjar, B., 2002b. Frameworks for finite strain viscoelastic-plasticity based on multiplicative decompositions. Part II: computational aspects. *Computer Methods in Applied Mechanics and Engineering* **191**, 1563–1593.
- Nedjar, B., 2007. An anisotropic viscoelastic fibre-matrix model at finite strains: Continuum formulation and computational aspects. *Computer Methods in Applied Mechanics and Engineering* **196**(9-12), 1745–1756.
- Nedjar, B., 2011. On a continuum thermodynamics formulation and computational aspects of finite growth in soft tissues. *International Journal for Numerical Methods in Biomedical Engineering* **27**, 1850–1866.
- Nedjar, B., 2013a. Formulation of a nonlinear porosity law for fully saturated porous media at finite strains. *Journal of the Mechanics and Physics of Solids* **61**(2), 537–556.
- Nedjar, B., 2013b. Poromechanics approach for modeling closed-cell porous materials with soft matrices. *International Journal of Solids and Structures* **50**, 3184–3189.
- Nedjar, B., 2014. On finite strain poroplasticity with reversible and irreversible porosity laws. Formulation and computational aspects. *Mechanics of Materials* **68**, 237–252.
- Ogden, R., 1997. *Non-linear Elastic Deformations*. Dover, New York.
- Pao, Y., 1978. Electromechanic forces in deformable continua. In: Nemat-Nasser, S. (Ed.), *Mechanics Today*, vol. 4. Oxford University Press, pp. 209–305.

- Simo, J., 1998. Numerical analysis and simulation of plasticity. In: Ciarlet, P., Lions, J. (Eds.), *Handbook of Numerical Analysis*, vol. VI. North-Holland, pp. 183–499.
- Simo, J., Hughes, T., 1998. *Computational Inelasticity*. Springer-Verlag, New York.
- Spencer, A., 1984. Constitutive theory for strongly anisotropic solids. In: Spencer, A. (Ed.), *Continuum Theory of the Mechanics of Fibre-reinforced Composites*, CISM Courses and Lectures No. 282. Springer, Wien.
- Steigmann, D., 2004. Equilibrium theory for magnetic elastomers and magnetoelastic membranes. *International Journal of Non-Linear Mechanics* **39**, 1193–1216.
- Truesdell, C., Noll, W., 1965. The nonlinear field theories of mechanics. In: Fluegge, S. (Ed.), *Handbuch der Physik Bd. III/3*. Springer-Verlag, Berlin.
- Varga, Z., Filipcsei, G., Zrínyi, M., 2006. Magnetic field sensitive functional elastomers with tunable elastic modulus. *Polymer* **47**, 227–233.
- Vu, D., Steinmann, P., 2007. Nonlinear electro- and magneto-elastostatics: material and spatial settings. *International Journal of Solids and Structures* **44**, 7891–7901.
- Wilmanski, K., 2003. On thermodynamics of nonlinear poroelastic materials. *Journal of Elasticity* **71**, 247–261.
- Wriggers, P., 2008. *Nonlinear Finite Element Methods*. Springer-Verlag, Berlin, Heidelberg.

- Zhao, X., Kim, J., Cezar, C., Huebsch, N., Lee, K., Bouhadir, K., Mooney, D., 2011. Active scaffolds for on-demand drug and cell delivery. *Proceedings of the National Academy of Sciences (PNAS)* **108**(1), 67–72.
- Zienkiewicz, O., Taylor, R., 2000. *The Finite Element Method*, 5th Ed., Volume 1. Butterworth-Heinemann, Oxford, UK.
- Zrínyi, M., Barsi, L., Büki, A., 1996. Deformation of ferrogels induced by nonuniform magnetic fields. *Journal of Chemical Physics* **104**(21), 8750–8756.